

José Lukas Montenegro Ferreira

Time Rescaling as a Shortcut to Adiabatic Population Transfer in Quantum Three-level Systems

João Pessoa, PB - Brazil

July, 2024

José Lukas Montenegro Ferreira

Time Rescaling as a Shortcut to Adiabatic Population Transfer in Quantum Three-level Systems

Dissertation submitted to the graduate program in physics of the Federal University of Paraíba, as part of the requirements to obtain the degree of Master in Physics (MPHYS).

Federal University of Paraíba

Physics Department

Graduate Program in Physics

Supervisor: Bertúlio de Lima Bernardo

Co-supervisor: Alexandre da Silva Rosas

João Pessoa, PB - Brazil

July, 2024

Catálogo na publicação
Seção de Catalogação e Classificação

F383t Ferreira, José Lukas Montenegro.

Time rescaling as a shortcut to adiabatic population transfer in quantum three-level systems / José Lukas Montenegro Ferreira. - João Pessoa, 2024.

77 f. : il.

Orientação: Bertúlio de Lima Bernardo.

Coorientação: Alexandre da Silva Rosas.

Dissertação (Mestrado) - UFPB/CCEN.

1. Atalhos para adiabaticidade. 2. Dinâmica quântica. 3. Física atômica. 4. Inversão de população. I. Bernardo, Bertúlio de Lima. II. Rosas, Alexandre da Silva. III. Título.

UFPB/BC


CDU 53(043)




Universidade Federal da Paraíba
Centro de Ciências Exatas e da Natureza
Programa de Pós-Graduação *Stricto Sensu* em Física

Ata da Sessão Pública da Defesa de dissertação de **Mestrado** do aluno **José Lukas Montenegro Ferreira**, candidato ao Título de Mestre em Física na Área de Concentração Física da Matéria Condensada.


Aos vinte e seis dias do mês de julho do ano de dois mil de vinte e quatro, às 09h00, na sala virtual <https://meet.google.com/okz-padc-adj>, reuniram-se os membros da Banca Examinadora constituída para avaliar a dissertação de Mestrado, na área de Física da Matéria Condensada, de **José Lukas Montenegro Ferreira**. A banca foi composta pelos(as) professores(as) doutores(as): Bertúlio de Lima Bernardo (UFPB), orientador e presidente da banca examinadora, Alexandre da Silva Rosas (UFPB), coorientador, Thierry Marcelino Passerat de Silans (UFPB) e Marcus Vinicius Segantini Bonança (UNICAMP). Dando início aos trabalhos, o Prof. Bertúlio de Lima Bernardo comunicou aos presentes a finalidade da reunião. A seguir, passou a palavra para o candidato para que o mesmo fizesse, oralmente, a exposição da pesquisa de dissertação intitulada “*Reescalonamento temporal como um atalho para transferência adiabática de população em sistemas quânticos de três níveis*”. Concluída a exposição, o candidato foi arguido pela Banca Examinadora, que emitiu o parecer “**aprovado**”. Assim sendo, deve a Universidade Federal da Paraíba expedir o respectivo diploma de Mestre em Física na forma da lei. E para constar, Ana Beatriz Cândido Vieira, Assistente em Administração, redigiu a presente ata que vai assinada pelos membros da Banca Examinadora. João Pessoa, Paraíba, **26 de julho de 2024**.

Documento assinado digitalmente
 **BERTULIO DE LIMA BERNARDO**
Data: 26/07/2024 14:27:23-0300
Verifique em <https://validar.iti.gov.br>


Prof. Dr. Bertúlio de Lima Bernardo
Orientador - PPGF/UFPB

Documento assinado digitalmente
 **THIERRY MARCELINO PASSERAT DE SILANS**
Data: 26/07/2024 19:42:01-0300
Verifique em <https://validar.iti.gov.br>

Prof. Dr. Thierry Marcelino Passerat de Silans
PPGF/UFPB

Documento assinado digitalmente
 **ALEXANDRE DA SILVA ROSAS**
Data: 28/07/2024 18:51:59-0300
Verifique em <https://validar.iti.gov.br>

Prof. Dr. Alexandre da Silva Rosas
Coorientador - PPGF/UFPB

Documento assinado digitalmente
 **MARCUS VINICIUS SEGANTINI BONANCA**
Data: 28/07/2024 18:06:14-0300
Verifique em <https://validar.iti.gov.br>

Prof. Dr. Marcus Vinicius Segantini Bonança
UNICAMP

Acknowledgements

I would like to begin by thanking my parents, Jailson and Tereza, for all their encouragement and support over these years of studies, both during undergraduate and graduate levels. Not only their love for me, but also their acknowledgement of the importance of the development of science, must be praised. Similar thanks go to the rest of my family and relatives.

I would like also to thank professor Dr. Bertúlio de Lima Bernardo, my supervisor, for these more than five years of partnership and guidance. His unwavering support was an essential element of my development as student and researcher, as well as that of professor Dr. Alexandre Rosas, my co-supervisor. I would also like to thank professor Dr. Jesus Pavon Lopez, for the many informative conversations on the experimental aspects of my work. The other teachers and staff at the Physics Department of the Federal University of Paraíba, deserve thanks for their help in my intellectual development.

My friends Rennan, Rafaelly, Carlos and so many others have been a fundamental part of my path, with their friendship, curiosity for my work and encouragement, and deserve a special thanks. A mention must also be made for Dr. Ângelo França, for the many discussions we had, as well as the preparation of many of the plots used both in this work and in the paper we published together. Additional thanks goes to the members of the committee in charge of evaluating this work. Your hours of commitment to read, consider and propose changes and improvements are appreciated.

A final acknowledgment goes to the *Coordenação de Aperfeiçoamento de Pessoal de Nível Superior* (CAPES), for the financial support during these two years of graduate studies.

"I think it is not an exaggeration to say that the (...) clarification of the quantum description of single objects have been at the root of a second quantum revolution, and that John Bell was its prophet. And it may well be that this once purely intellectual pursuit will also lead to a new technological revolution."

(Alain Aspect)

Abstract

The promotion of efficient population inversion in single quantum systems is a useful tool in quantum information and quantum computation sciences, since it allows for the precise preparation of states and the construction of logical gates such as the Hadamard. In this work we present a protocol to accelerate the population inversion in three-level atomic systems, by using the time rescaling (TR) shortcut to adiabaticity to speed up the STIRAP (Stimulated Raman Adiabatic Passage) protocol. We also show that the TR method follows the same path as the reference protocol, meaning that, if the reference protocol is an adiabatic dynamics, the shortcut to adiabaticity obtained via the TR method is transitionless, similar to the one obtained from the Counterdiabatic method. This introduces simplifications in our evaluation. Finally, we discuss the fidelity and thermodynamic cost of the protocol.

Keywords: STIRAP; shortcuts to adiabaticity; time rescaling method; population inversion; quantum dynamics; transitionless driving;

List of Figures

Figure 1 – Transporting a pendulum inside a box very slowly, allows to maintain it oscillating in the same amplitude. ‘The slowness’ is a tool for control. This is the idea behind the adiabatic theorem. Image extracted from (GRIFFITHS, 2019).	26
Figure 2 – Populations of the levels $ 1\rangle$ (blue), $ 2\rangle$ (black) and $ 3\rangle$ (red) of an atomic system during a process of population transfer through the (a) reference protocol in non-adiabatic time, and (b) counterdiabatic protocol. Extracted from (LI; CHEN, 2016).	30
Figure 3 – Semi-classical model of interaction between a molecular system and an external (pump) radiation field of frequency ν_p . (a) Stokes Raman scattering: energy is absorbed from the pump and, upon emission, part is kept in form of vibrational energy, so that $\nu_s < \nu_p$. (b) Rayleigh (elastic) scattering: no energy is retained by the molecule, $\nu_s = \nu_p$. (c) Anti-Stokes Raman scattering: energy is absorbed from the pump and, upon emission, part of the original vibrational energy is lost to the exiting radiation ($\nu_{as} > \nu_p$).	34
Figure 4 – Conceptual schematics of a Λ three-level atomic system, under the influence of external Stokes and pump laser pulses of respective Rabi frequencies $\Omega_s(t)$ and $\Omega_p(t)$. The solid lines represent the undisturbed atomic energy levels, while dashed lines represent the virtual levels. The detuning of the Stokes and the pump fields with respect to the real atomic levels are given by Δ_s and Δ	36
Figure 5 – Time behavior of: (a) the pump (blue) and stokes (red) pulses given by equations (4.34) and (4.35), and (b) the populations of the atomic levels $ 1\rangle$ (blue), $ 2\rangle$ (purple) and $ 3\rangle$ (red), with the initial state given by $ n_0(0)\rangle \approx 1\rangle$. The parameters used are specified in the text.	48
Figure 6 – Time behavior of a general reference process, $a = 1$, and the designed TR processes for $a = 2$ and $a = 10$. The route followed by the quantum system from the initial state $ \psi_i\rangle$ to the final state $ \psi_f\rangle$ through the Hilbert space is the same in all cases. However, the time necessary to reach any state $ \psi_\gamma\rangle$ of the route can be made shorter with increasing a	53
Figure 7 – Behavior of the new pump (blue) and stokes (red) pulses, with the contraction parameter assuming the values of (a) $a = 2$ and (b) $a = 10$. The same parameters of fig. 5 were used. Although the plots closely resemble Gaussian shapes, they are modulated as given in equations (5.14a) and (5.14b).	58

Figure 8 – Time evolution of the populations of levels $ 1\rangle$ (blue), $ 2\rangle$ (dashed purple) and $ 3\rangle$ (red) for the TR passage protocol with the initial state given by $ 1\rangle$, and the contraction parameter assuming the values (a) $a = 2$ and (b) $a = 10$. In both cases we observe that the population inversion occurs at least a times faster than in the reference ($a = 1$) protocol, shown in fig. 5. The same parameters of fig. 5 were considered.	59
Figure 9 – Probability transfer to state $ 3\rangle$ as a function of the delay between pulses, for pulse areas of (a) 5π , (b) 10π , (c) 15π and (d) 20π . Gaussian pulses in the form described in eqs. (4.34) and (4.35) were used, with $\Delta = 0$. Observe that in all cases, there is a wide plateau within which the protocol is performed with high fidelity, regardless of changes in the delay. Image taken from (SHORE, 2017).	60
Figure 10 – Behavior of the fidelity of the TR STIRSAP (blue) and counterdiabatic STIRSAP (red) against errors in the separation time between pulses. We used the same parameters of fig. 5, with the exception of the original t_0 of the counterdiabatic protocol, taken as $t_0 = t_f/8$ for optimization.	62
Figure 11 – Behavior of the fidelity of the TR STIRSAP (blue), counterdiabatic STIRSAP (red) and direct two-level population inversion via π pulse (black) for (a) variations in the amplitude of the pulses and (b) variations in the one-photon detuning. The same parameters of fig. 10 were used.	63

Contents

1	INTRODUCTION	13
2	THEORETICAL FOUNDATIONS	17
2.1	Quantum Dynamics	17
2.2	Semi-classical Model for Light-Matter Interaction	19
3	SHORTCUTS TO ADIABATICITY	23
3.1	Adiabatic Theorem	23
3.2	Shortcuts to Adiabaticity	26
3.3	Counterdiabatic Driving	27
3.4	Time-rescaling as a STA	30
4	STIRAP PROTOCOL	33
4.1	Raman Scattering	33
4.2	General idea of the STIRAP Protocol	35
4.3	Rotating Wave Approximation Hamiltonian	35
4.4	Eigenvalues and Eigenstates	39
4.5	Special Conditions for the STIRAP	43
4.6	Performing the STIRAP	46
5	RESULTS	51
5.1	Transitionless Proof	51
5.1.1	Analysis of the Evolution created by the TR Hamiltonian	51
5.1.2	Transitionless Proof via the Adiabatic Theorem	53
5.2	Performing the STIRSAP	55
5.3	Stability Against Errors	59
5.4	Thermodynamic Cost	63
5.4.1	Two-point Measurement Method	63
5.4.2	Evaluation of Cost for Reference and TR Protocols	67
6	CONCLUSION	69
	BIBLIOGRAPHY	71

1 Introduction

One of the great revolutions in quantum mechanics was the development of techniques to manipulate individual quantum systems in a controlled way (CHEN; WANG; ZHOU, 2021; RAIMOND; BRUNE; HAROCHE, 2001). This, in turn, resulted in the emergence of several technologies, the most important of which, perhaps, is quantum computing. The operation of a quantum computer requires several controlled processes, such as the preparation of qubits (VOLYA; MISHRA, 2024), the construction of gates (SANTOS; D.; SARANDY, 2016) and the transport of information through qubit chains (YONEDA et al., 2021).

Among these techniques, adiabatic protocols are of particular interest. These protocols obey the adiabatic theorem, which guarantees (as it will be shown in section 3.1), that if the associated Hamiltonian varies sufficiently slow, the quantum system evolves in time while preserving certain properties. Specially, if the system is initially prepared in one of the eigenstates of this Hamiltonian, it remains in this same eigenstate throughout the process. This can be useful, for example, in moving ion traps, where keeping the system in its ground state at all times results in optimal transport, since excitation may lead atoms to escape the trap (COUVERT et al., 2008; FÜRST et al., 2014). Moreover, quantum computation can be performed entirely through adiabatic evolutions, the so-called “Adiabatic quantum computing (AQC)”, which was shown to be polynomially equivalent to the traditional circuit model of quantum computation (FARHI et al., 2000).

In spite of their importance, adiabatic protocols suffer from an inconvenient setback: they need to be executed in a long period of time, the adiabatic theorem is perfectly satisfied as the time of the protocol goes to infinity. This, in turn, allows for a prolonged interaction between the system and its environment, the result of which is decoherence, or the loss of its useful quantum properties (SANTOS et al., 2023) before the desired process is completed. As a rough example, in 2022 IBM announced a new 127-qubits quantum processor named Eagle, whose coherence time¹ was about $400\mu s$ (DIAL, 2022). If we were to execute individual operations such as population inversions (NOT gates) in this computer through adiabatic protocols, and each of them took only a few microseconds to run (WANG et al., 2013), this computer would be able to perform less than one hundred operations before losing its optimal coherence. This is a derisory amount when compared

¹ Coherence time is defined as the average time during which the system preserves its coherence (HECHT, 2017).

to the number of operations required to execute useful algorithms ².

To solve this impasse, several paths could be taken: for once, one could search for methods to better isolate the system, so that the coherence time would increase. Another way would be to seek for protocols that preserve the useful properties of the adiabatic dynamics, but without the same limitation of long time duration. This is the inspiration behind the creation of a series of techniques called “shortcuts to adiabaticity”, or STAs. Their general implementation involves a modification in the adiabatic Hamiltonian (by adding or modulating the original fields), so that the system is forced to remain at, or is brought back to the same final state as it would be by the associated adiabatic protocol (also called ‘reference’ protocol), but at necessarily faster times.

This work will make use of a particular STA, the so-called time rescaling (TR) method (BERNARDO, 2020). The main idea, as better explained in section 3.4, is to rescale the time parameter, turning it into a function $t = f(\tau)$. This results in a modification of the reference Hamiltonian which allows to speed up the reference protocol, in principle, as much as one wishes, by changing a time contraction parameter, a . From the many advantages of the time rescaling, such as not requiring a previous knowledge of the instantaneous eigenstates of the reference Hamiltonian, or being applicable to any type of reference protocol, not only adiabatic, it seemed until now to suffer from a disadvantage. Although guaranteeing that a system starting at a given eigenstate would be brought back to that same eigenstate, its route in Hilbert space during the evolution was unknown. The knowledge of the route is of paramount importance for properly understanding the dynamics of system; for example, it may allow for an analytic evaluation of the probabilities of finding the system in different eigenstates overtime. In contrast, a STA such as the counterdiabatic method (CD) has a known route - it guarantees the permanence of the system in that original eigenstate throughout the process. Protocols like the CD have **transitionless** routes. In this work we shall demonstrate which route is followed by systems driven by TR base protocols, and show that it belongs to this transitionless class of STAs.

The TR method will be used here as a STA to accelerate the Stimulated Raman Adiabatic Passage (STIRAP) protocol, an adiabatic technique used to promote population inversion between two-levels of a three-level system (SHORE, 2017). This technique was originally conceived to perform controlled population transfer between the vibrational energy levels of molecules (KUKLINSKI et al., 1989), but was soon extended to a wide variety of three-level systems (VITANOV et al., 2001; VITANOV et al., 2017). Here, we shall be concerned with the case of a three-level atomic system in a Λ linkage pattern, as

² To use Shor’s algorithm to factor a 1024-bit number, for example, we would need to execute about $\approx 10^{11}$ operations (YAMAGUCHI et al., 2023).

explained in section 4.2. The advantages of exploring this problem are both theoretical and practical.

From the theoretical standpoint, the TR method was already applied to the study of the two-level population inversion with considerable success (ANDRADE; FRANÇA; BERNARDO, 2022), and hence it seems a natural progression to explore the capacity of this approach in more complicated systems. For example, while in the two-level case, only one type of laser pulse is involved, in the execution of the STIRAP we have two lasers pulses, which must obey certain joint conditions such as proper ordering and separation time. Hence, by studying the acceleration of this protocol through the TR STA, we develop a bigger understanding of its capabilities and prepare to tackle even more complex problems.

From the practical standpoint, achieving population inversion in a two-level system model is not particularly used, due to the need to fight against spontaneous emission from the excited state. Hence, although interesting as a conceptual model, it is hardly used experimentally; the preference being for three or four-level systems (AGNESI; REALI, 2024). Also, certain direct transitions between two-levels are forbidden by selection rules (GRIFFITHS, 2019), an impediment that can be circumvented through the choice of a three-level system. Hence, by proposing a method to accelerate the STIRAP through the TR approach, we offer to the experimentalist a possible new and simple form of achieving feasible population inversions in a shorter time interval. This could potentially lead to the creation of more efficient single-qubit gates in ion or neutral atom-based quantum computers (BENENTI et al., 2019).

This work is divided in six chapters. The first, this introduction, offers a general contextualization of the problem being treated, and its importance. The second discusses some useful theoretical foundations, mostly associated with the semi-classical model of light-matter interaction. The third chapter concerns the adiabatic theorem, whose proof is presented in detail, as well as the concept of STA, two of which will be better explained: the counterdiabatic method and the time rescaling method. The fourth chapter presents a detailed description of the STIRAP protocol. In the fifth chapter, the results of this dissertation are presented. First, we prove by two different ways, that the time rescaling method is transitionless. This important result is applied next, by performing an acceleration of the STIRAP protocol and showing how the transitionless argument simplifies the assessment of the population inversion throughout the process. We discuss the differences of the accelerated protocol in terms of the reference one. The fidelity and thermodynamic cost to perform it, are also evaluated. We finish with chapter six, the conclusion, which makes a simple abridgment of what was discussed, and points out to future inquiries.

2 Theoretical Foundations

This chapter is dedicated to present certain fundamental theoretical tools that will be useful in subsequent chapters, but which would not fit well as subsections or digressions of the material being presented. They concern, mainly, with the semi-classical treatment of the interaction between matter and radiation under Schrödinger's formalism.

2.1 Quantum Dynamics

We consider an initial situation of a system under a time-independent Hamiltonian \hat{H}_0 , whose eigenvalues, E_n , and eigenstates, $|n\rangle$, are known and obey the relation,

$$\hat{H}_0 |n\rangle = E_n |n\rangle. \quad (2.1)$$

Now, let us suppose that a time-dependent Hamiltonian, $\hat{V}(t)$, which acts as a perturbation in the system, is turned on. The new Hamiltonian generating the time evolution is now,

$$\hat{H}(t) = \hat{H}_0 + \hat{V}(t), \quad (2.2)$$

and if the general state is originally defined as,

$$|\psi\rangle = \sum_n c_n |n\rangle e^{-i\xi_n(t)}, \quad (2.3)$$

with ξ_n 's being phases to be determined later, the evolution state can still be written in terms of $\{|n\rangle\}$, since it forms a complete set. The amplitudes, however, now become functions of time ([ZWIEBACH, 2018](#); [SHANKAR, 1994](#)),

$$|\psi\rangle = \sum_n c_n(t) |n\rangle e^{-i\xi_n(t)}. \quad (2.4)$$

The effect of the perturbation will be, then, to allow ‘transitions’ between the eigenstates ([COURTEILLE, 2023](#); [GRIFFITHS, 2019](#)). The application of equation (2.4)

in the Schrödinger equation yields,

$$\begin{aligned}
 i\hbar \frac{d}{dt} \left[\sum_n c_n(t) |n\rangle e^{-i\xi_n(t)} \right] &= [\hat{H}_0 + \hat{V}(t)] \sum_n c_n(t) |n\rangle e^{-i\xi_n(t)}, \\
 i\hbar \left[\sum_n \dot{c}_n(t) |n\rangle e^{-i\xi_n(t)} - i \sum_n c_n(t) |n\rangle e^{-i\xi_n(t)} \dot{\xi}_n(t) \right] &= \sum_n c_n(t) E_n |n\rangle e^{-i\xi_n(t)} \\
 &\quad + \sum_n c_n(t) \hat{V}(t) |n\rangle e^{-i\xi_n(t)}.
 \end{aligned} \tag{2.5}$$

Now, applying $\langle m|$ on both sides, we get

$$[i\hbar \dot{c}_m(t) + \hbar c_m(t) \dot{\xi}_m(t)] e^{-i\xi_m(t)} = c_m(t) E_m e^{-i\xi_m(t)} + \sum_n c_n(t) \langle m| \hat{V}(t) |n\rangle e^{-i\xi_n(t)},$$

$$i\hbar \dot{c}_m(t) + \hbar c_m(t) \dot{\xi}_m(t) = c_m(t) E_m + \sum_n c_n(t) \langle m| \hat{V}(t) |n\rangle e^{i[\xi_m(t) - \xi_n(t)]},$$

and finally, we obtain the following coupled equations,

$$i\hbar \dot{c}_m(t) = [E_m - \hbar \dot{\xi}_m(t) + V_{mm}(t)] c_m(t) + \sum_{n \neq m} c_n(t) V_{mn}(t) e^{i[\xi_m(t) - \xi_n(t)]}. \tag{2.6}$$

Since our interest will be in three-level systems, it is useful to write down equation (2.6) for this case. In matrix form, it is written as

$$\begin{pmatrix} \dot{c}_1(t) \\ \dot{c}_2(t) \\ \dot{c}_3(t) \end{pmatrix} = \frac{-i}{\hbar} \begin{pmatrix} E_1 - \hbar \dot{\xi}_1(t) + V_{11}(t) & V_{12} e^{-i(\xi_2 - \xi_1)} & V_{13} e^{-i(\xi_3 - \xi_1)} \\ V_{21} e^{i(\xi_2 - \xi_1)} & E_2 - \hbar \dot{\xi}_2(t) + V_{22}(t) & V_{23} e^{-i(\xi_3 - \xi_2)} \\ V_{31} e^{i(\xi_3 - \xi_1)} & V_{32} e^{i(\xi_3 - \xi_2)} & E_3 - \hbar \dot{\xi}_3(t) + V_{33}(t) \end{pmatrix} \begin{pmatrix} c_1 \\ c_2 \\ c_3 \end{pmatrix}. \tag{2.7}$$

Equation (2.7) describes the time evolution of the amplitudes of the the general state, whose solution depends on the specific Hamiltonian involved. The square modulus of these amplitudes yield the time-dependent probabilities of finding the system in each of the eigenstates of the undisturbed Hamiltonian or, for an ensemble of equally prepared systems, the populations of each of the three levels as a function of time,

$$P_1(t) = |c_1(t)|^2, \tag{2.8a}$$

$$P_2(t) = |c_2(t)|^2, \tag{2.8b}$$

$$P_3(t) = |c_3(t)|^2. \tag{2.8c}$$

2.2 Semi-classical Model for Light-Matter Interaction

To solve the dynamical equations of the previous section, the interaction Hamiltonian must be determined. Since our focus will be in atomic systems, we start considering that, without perturbations, a hydrogen-like atom would have a Hamiltonian which depends only on the position and momentum of the electron with respect to the nucleus,

$$\hat{H}_0(\mathbf{r}) = \frac{\hat{\mathbf{p}}^2}{2m} + U(\mathbf{r}), \quad (2.9)$$

with $U(\mathbf{r})$ being the Coloumb electric potential. The spectrum of energy and respective eigenstates for such system are well known¹ (SHANKAR, 1994). Now, if an external perturbation $\hat{V}(t)$, in the form of electromagnetic radiation, is “turned on”, we have a change in the Hamiltonian, which becomes (JACKSON, 1998)

$$\hat{H}(\mathbf{r}, t) = \frac{1}{2m}[\hat{\mathbf{p}} + e\mathbf{A}(\mathbf{r}, t)]^2 - e\Phi(\mathbf{r}, t) + U(\mathbf{r}), \quad (2.10)$$

with e being the electric charge, and $\mathbf{A}(\mathbf{r}, t)$ and $\Phi(\mathbf{r}, t)$ the vector and scalar potentials, respectively. We also make some impositions: i) the Weyl gauge (HAYASHI; KUGO, 1979) ($\Phi = 0$), and ii) under the dipole approximation², $\mathbf{A}(\mathbf{r}, t) = \mathbf{A}(t)$ (BOSSMANN; GRUMMT; MARTIN, 2018). Equation (2.10), then, becomes

$$\hat{H}(\mathbf{r}, t) = \frac{1}{2m}[\hat{\mathbf{p}} + e\mathbf{A}(t)]^2 + U(\mathbf{r}). \quad (2.11)$$

It is important now to notice that in the electromagnetic theory, the true observable quantities are the electric and magnetic fields, so that the potentials can be transformed (gauge transformations), as long as the fields are maintained invariant. By means of the transformation (GENES, 2007)

$$\chi(r, t) = -\mathbf{A}(t) \cdot \mathbf{r}, \quad (2.12)$$

we obtain the new scalar and vector potentials,

¹ even in the case of many-electrons' systems, the energy corrections only depend on the coordinates.

² In interactions between atoms and radiation, since we restrict our problem to situations where $\lambda \gg R_{atom}$, we can assume that the spatial part of the electric field function (and of the associated potential functions) are real amplitudes of constant value.

$$\Phi'(\mathbf{r}, t) = \Phi(\mathbf{r}, t) - \frac{\partial \chi(\mathbf{r}, t)}{\partial t} = \mathbf{r} \cdot \mathbf{E}(t), \quad (2.13a)$$

and,

$$\mathbf{A}'(\mathbf{r}, t) = \mathbf{A}(\mathbf{r}, t) + \nabla \chi(\mathbf{r}, t) = 0. \quad (2.13b)$$

The new Hamiltonian is then

$$\hat{H}(\mathbf{r}, t) = \frac{1}{2m} [\hat{\mathbf{p}} + e\mathbf{A}'(\mathbf{r}, t)]^2 + U(\mathbf{r}) - e\Phi'(\mathbf{r}, t), \quad (2.14)$$

$$\hat{H}(\mathbf{r}, t) = \left[\frac{\hat{\mathbf{p}}^2}{2m} + U(\mathbf{r}) \right] - e\mathbf{r} \cdot \mathbf{E}(t). \quad (2.15)$$

If we compare equations (2.15) and (2.9), we obtain

$$\hat{V}(t) = -\mathbf{d} \cdot \mathbf{E}(t), \quad (2.16)$$

where \mathbf{d} is the electric dipole moment, defined as $\mathbf{d} = e\mathbf{r}$.

So far, we have been using implicitly a semi-classical model to describe the light-matter interaction. This means that the atomic observables are quantized, but the radiation fields are treated classically. In this model, the electric field can be written as

$$\mathbf{E}(t) = \frac{\mathcal{E}}{2} (e^{i\omega t} + e^{-i\omega t}) \hat{\epsilon}, \quad (2.17)$$

\mathcal{E} being the amplitude of the field, ω its angular frequency of oscillation, and $\hat{\epsilon}$, the polarization unit vector. Also, since neutral atoms have no permanent electric dipole moment (GENES, 2007), the diagonal elements of the electric dipole matrix are null. The off-diagonal terms can be different from zero, however, and this ‘remanescent’ dipole can couple with the electric field of the external radiation to promote transitions between states. This particular kind of dipole only exists in quantum mechanics, and is called ‘transition dipole moment’ (BRASLAVISKY, 2007).

Now, by applying (2.17) into (2.16), the elements of the interaction matrix are obtained as,

$$\langle i | \hat{V}(t) | j \rangle = -\langle i | \mathbf{d} \cdot \mathbf{E}(t) | j \rangle =$$

$$= -\langle i | \frac{\hbar e \mathcal{E} \mathbf{d} \cdot \hat{\epsilon}}{2} (e^{i\omega t} + e^{-i\omega t}) | j \rangle ,$$

$$\langle i | \hat{V}(t) | j \rangle = V_{ij}(t) = \frac{\hbar \Omega_{ij}}{2} (e^{i\omega t} + e^{-i\omega t}). \quad (2.18)$$

The term Ω_{ij} introduced above will be of great importance to the subsequent discussions. It is called ‘Rabi frequency’, which is defined as

$$\Omega_{ij} = -\frac{e \mathcal{E}}{\hbar} \langle i | \mathbf{d} \cdot \hat{\epsilon} | j \rangle . \quad (2.19)$$

The origin of the term is associated to the fact that, when treating two-level atomic systems in a semi-classical Rabi model, Ω_{ij} is the frequency that the electron oscillates between levels i and j .

Before ending this section, it is important to strengthen the physical understanding behind the mathematical developments made so far. When an atom is in a lower energy level $|i\rangle$, it can absorb the necessary $(E_j - E_i)$ energy from the external radiation field to be promoted to a higher energy level, $|j\rangle$. Once in this level, it can be stimulated to release energy in the same quantity to the field, and return to the lower level, $|i\rangle$. From quantum theory, the probability of absorption and stimulated emission are equal (FOX, 2006). These transitions are possible due to the coupling of the transition dipole moment of the atom with the electric field of the external radiation. This model is of particular importance, since it allows the use of external radiation fields (such as lasers) to precisely prepare atomic systems in a given configuration.

3 Shortcuts to Adiabaticity

In this section we shall discuss the recently developed protocols known as shortcuts to adiabaticity, or STAs. As the name suggests, the aim of these protocols is to produce time-evolution in quantum systems that conserve the properties of an adiabatic dynamics, but faster. We begin by exposing the ‘adiabatic theorem’, and what are the benefits of an adiabatic dynamics. We then introduce the formal concept of STA, with some examples. The counterdiabatic driving, which is arguably the most famous STA method, is then explored in some detail, followed by the time-rescaled dynamics, which is the STA approach to be used in subsequent sections.

3.1 Adiabatic Theorem

The adiabatic theorem ([BORN; FOCK, 1928](#); [KATO, 2021](#)) is one of the most useful approximation methods in quantum mechanics. To understand its importance, we begin by considering a time-dependent Hamiltonian, whose instantaneous eigenvalues and eigenstates are given by the eigenvalue equation ([GRIFFITHS, 2019](#)),

$$\hat{H}(t) |n(t)\rangle = E_n(t) |n(t)\rangle. \quad (3.1)$$

A general state representing a N-level quantum system can be described by a superposition of these eigenstates,

$$|\psi(t)\rangle = \sum_n c_n(t) |n(t)\rangle e^{i\theta_n(t)t}, \quad (3.2)$$

where $\theta_n(t)$ the so called “dynamical phase”, which is given by

$$\theta_n(t) = -\frac{1}{\hbar} \int_0^t E_n(t') dt'. \quad (3.3)$$

The evolution of the state in equation (3.2) is given by the Schrödinger equation, such that, by applying equation (3.2) to it, we obtain

$$i\hbar \frac{d}{dt} \left(\sum_n c_n(t) |n(t)\rangle e^{i\theta_n(t)t} \right) = \hat{H} \left(\sum_n c_n(t) |n(t)\rangle e^{i\theta_n(t)t} \right),$$

From which we find,

$$i\hbar \sum_n \left(\dot{c}_n(t) |n(t)\rangle + c_n(t) |\dot{n}(t)\rangle + c_n(t) |n(t)\rangle \dot{\theta}_n(t) \right) e^{i\theta_n t} = \sum_n c_n(t) E_n(t) |n(t)\rangle e^{i\theta_n t}, \quad (3.4)$$

with $|\dot{n}(t)\rangle = \frac{d}{dt} |n(t)\rangle$. The last term of the left-hand side of (3.4), becomes, by using equation (3.3),

$$i\hbar \sum_n i c_n(t) |n(t)\rangle e^{i\theta_n t} \frac{d}{dt} \left(-\frac{1}{\hbar} \int_0^t E_n(t') dt' \right) = \sum_n c_n(t) |n(t)\rangle E_n(t) e^{i\theta_n t},$$

which cancels out with the right-hand side of equation (3.4). Hence, we are left with

$$\sum_n \dot{c}_n(t) |n(t)\rangle e^{i\theta_n t} = - \sum_n c_n(t) |\dot{n}(t)\rangle e^{i\theta_n t}. \quad (3.5)$$

By applying $\langle m(t)|$ on both sides of equation (3.5), we obtain the series of coupled equations,

$$\sum_n \dot{c}_n(t) \langle m(t)|n(t)\rangle e^{i\theta_n(t)} = \dot{c}_m(t) e^{i\theta_m(t)} = - \sum_n c_n(t) \langle m(t)|\dot{n}(t)\rangle e^{i\theta_n t},$$

which provides,

$$\dot{c}_m(t) = -c_m(t) \langle m(t)|\dot{m}(t)\rangle - \sum_{n \neq m} c_n(t) \langle m(t)|\dot{n}(t)\rangle e^{i(\theta_n - \theta_m)}. \quad (3.6)$$

To proceed further, the inner products of the second term of the right-side of equation (3.6) can be re-written in a convenient manner, by differentiating equation (3.1), then applying $\langle m(t)|$ ($m \neq n$) on both sides to obtain

$$\dot{\hat{H}} |n(t)\rangle + \hat{H} |\dot{n}(t)\rangle = \dot{E}_n |n(t)\rangle + E_n |\dot{n}(t)\rangle,$$

$$\langle m(t)| \dot{\hat{H}} |n(t)\rangle + \langle m(t)| \hat{H} |\dot{n}(t)\rangle = \langle m(t)| \dot{E}_n |n(t)\rangle + \langle m(t)| E_n |\dot{n}(t)\rangle,$$

$$\langle m(t)| \dot{\hat{H}} |n(t)\rangle + E_m \langle m(t)|\dot{n}(t)\rangle = \dot{E}_n \langle m(t)|n(t)\rangle + E_n \langle m(t)|\dot{n}(t)\rangle,$$

and consequently,

$$\langle m(t) | \dot{n}(t) \rangle = \frac{\langle m(t) | \dot{\hat{H}} | n(t) \rangle}{E_n - E_m}, \quad (3.7)$$

where we made use of the orthogonality of the eigenstates and the Hermiticity of the Hamiltonian operator. By using equation (3.7) to reorganise equation (3.6), we arrive at,

$$\dot{c}_m(t) = -c_m(t) \langle m(t) | \dot{n}(t) \rangle - \sum_{n \neq m} \frac{\langle m(t) | \dot{\hat{H}} | n(t) \rangle}{E_n - E_m} e^{i(\theta_n - \theta_m)}. \quad (3.8)$$

This development is, so far, exact. We now impose the adiabatic approximation (SAKURAI; NAPOLITANO, 2021): if,

$$\left| \frac{\langle m(t) | \dot{\hat{H}} | n(t) \rangle}{E_n - E_m} \right| \equiv \frac{1}{t'} \ll |\langle m(t) | \dot{n}(t) \rangle| \sim \frac{E_m}{\hbar}, \quad (3.9)$$

the second term in the right-side of equation (3.8) can be discarded, with equation (3.8) becoming,

$$\dot{c}_m(t) \approx -c_m(t) \langle m | \dot{m} \rangle, \quad (3.10)$$

and

$$c_m(t) = c_m(0) e^{i\gamma_m(t)}, \quad (3.11)$$

with (3.11), $\gamma_m(t) = i \int_0^t \langle m(t') | \dot{n}(t') \rangle dt'$, the so-called ‘geometric phase’. This final result summarizes the **adiabatic theorem**, that follows:

“[If] the time scale t' for changes in the Hamiltonian [is] very large compared with the inverse natural frequency of the associated eigenstate phase factor(...) a system that starts out in an eigenstate $|n(0)\rangle$ of $\hat{H}(0)$, remains in the eigenstate $|n(t)\rangle$ of $\hat{H}(t)$.” (SAKURAI; NAPOLITANO, 2021).

From the above statement, we observe that the adiabatic theorem establishes a powerful tool for the control of the dynamics of arbitrary quantum systems. A classical

analogy to this is that of transport of a pendulum inside a box, made very slowly, in order to keep it moving with the same amplitude (figure 1). Its usefulness is attested in several areas, such as efficient population transfer in atoms and molecules, electronic transport, manipulation of atomic traps, among others (DEMIRPLAK; RICE, 2009; MALINOVSKY; KRAUSE, 2001; POGGIANI G. Z. LI; TESTERA; WERTH, 1991; AVRON; SEILLER; YAFFE, 1987).

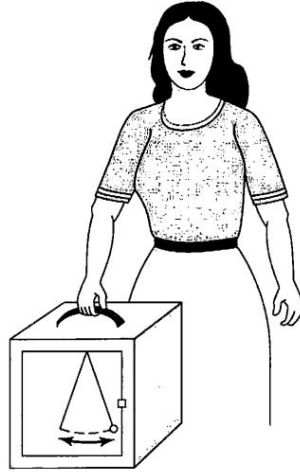


Figure 1 – Transporting a pendulum inside a box very slowly, allows to maintain it oscillating in the same amplitude. ‘The slowness’ is a tool for control. This is the idea behind the adiabatic theorem. Image extracted from (GRIFFITHS, 2019).

3.2 Shortcuts to Adiabaticity

In the previous subsection, the adiabatic theorem was presented as a tool for controlling the dynamics of a quantum system through a slow-varying Hamiltonian. Although notably useful, there are certain limitations associated to its application: the long process times required to perform any adiabatic protocol also permit a longer interaction between the system and its environment, resulting in undesirable effects such as noise, decoherence, dephasing and particle loss (SCHLOSSHAUER, 2007; SANTOS et al., 2023; SUTER; ALVAREZ, 2016).

To counter these undesirable effects, a series of methods collectively called *Shortcuts to Adiabaticity* (or STAs) were recently proposed (CHEN et al., 2010). STA protocols are dynamics which preserve the desirable properties of adiabatic transformations, but performed in a much shorter time (GUÉRY-ODELIN et al., 2019; YIN et al., 2022). This can be done in a variety of ways, and among the many examples of STAs in the literature,

we mention the *Counterdiabatic or transitionless quantum driving* (CD) (DEMIRPLAK; RICE, 2009; BERRY, 2009), the *fast-forward* protocol (TORRONTGUI et al., 2013), the *tunable-Hamiltonian* method (FRANÇA; ANDRADE; BERNARDO, 2022) and the *time rescaling dynamics* (TR) (BERNARDO, 2020). Both the CD and TR methods will be discussed in detail in the next subsections.

It is important to mention that, although primarily focused on speeding up the adiabatic dynamics of certain quantum mechanical systems, applications of the STAs were extended to several other areas of physics such as optical devices, classical mechanical systems, and even some posing questions in engineering (GUÉRY-ODELIN et al., 2019; LAKEHAL; MAAMACHE; CHOI, 2016; TORRONTGUI, 2017).

3.3 Counterdiabatic Driving

The counterdiabatic or transitionless quantum driving (abbreviated as CD) was the first proposed STA protocol, and currently the most widely used. As such, it is natural that any subsequent protocols appearing in the literature will be compared to it in terms of robustness and efficiency. Hence, it becomes important to discuss it here in some detail, before turning to the actual method to be applied in this work.

There are two main formulations of the CD protocol: one by Demirplak and Rice (DEMIRPLAK; RICE, 2009), and an independent one by Berry (BERRY, 2009). Our presentation here follows the later. We begin by considering a reference Hamiltonian $\hat{H}_0(t)$, which can be written as

$$\hat{H}_0(t) = \sum_n E_n(t) |n(t)\rangle \langle n(t)|, \quad (3.12)$$

in the basis of its instantaneous eigenstates. Now, if the initial state of the system is $|\psi(0)\rangle = |n(0)\rangle$, the adiabatic theorem discussed in section 3.1 guarantees that, to a slowly varying $\hat{H}_0(t)$, the state of the system evolves to

$$|\psi(t)\rangle \approx e^{i\sigma_n(t)} |n(t)\rangle, \quad (3.13)$$

meaning that it remains approximately in the same instantaneous eigenstate, apart from a phase factor $\sigma_n(t) = \theta_n(t) + \gamma_n(t)$.

Now, the counterdiabatic protocol consists in adding an auxiliary Hamiltonian (or CD Hamiltonian), $\hat{H}_{CD}(t)$, to ‘force’ the system to remain (and consequently arrive) precisely in the final state of (3.13), regardless of how fast the evolution of the Hamiltonian occurs. This means that the new Hamiltonian $\hat{H}(t)$ must satisfy the Schrödinger equation,

$$i\hbar \frac{\partial}{\partial t} |\psi(t)\rangle = \hat{H}(t) |\psi(t)\rangle. \quad (3.14)$$

Since the time-evolution of a closed quantum state can be described in terms of a unitary¹ time-evolution operator $\hat{\mathcal{U}}(t)$, satisfying

$$|\psi(t)\rangle = \hat{\mathcal{U}}(t) |\psi(0)\rangle, \quad (3.15)$$

we can re-write equation (3.14) as,

$$i\hbar \frac{\partial}{\partial t} \hat{\mathcal{U}}(t) |\psi(0)\rangle = \hat{H}(t) \hat{\mathcal{U}}(t) |\psi(0)\rangle,$$

$$i\hbar \frac{\partial}{\partial t} \hat{\mathcal{U}}(t) = \hat{H}(t) \hat{\mathcal{U}}(t).$$

Now, we apply the hermitian adjoint of the time evolution operator $\hat{\mathcal{U}}(t)$, $\hat{\mathcal{U}}^\dagger(t)$, on both sides, to obtain

$$i\hbar \frac{\partial}{\partial t} \hat{\mathcal{U}}(t) \hat{\mathcal{U}}^\dagger(t) = \hat{H}(t) \hat{\mathcal{U}}(t) \hat{\mathcal{U}}^\dagger(t),$$

$$\hat{H}(t) = i\hbar \left[\frac{\partial}{\partial t} \hat{\mathcal{U}}(t) \right] \hat{\mathcal{U}}^\dagger(t). \quad (3.16)$$

From equation (3.15), the time-evolution operator can be represented by

$$\hat{\mathcal{U}}(t) = \sum_n e^{i\sigma_n(t)} |n(t)\rangle \langle n(0)|, \quad (3.17)$$

and by applying equation (3.17) into equation (3.16), we obtain

$$\hat{H}(t) = i\hbar \left(\sum_n e^{i\sigma_n(t)} |\dot{n}(t)\rangle \langle n(0)| + i\dot{\sigma}_n(t) |n(t)\rangle \langle n(0)| \right) \sum_m e^{-i\sigma_m(t)} |m(0)\rangle \langle m(t)| =$$

¹ A unitary operator \hat{A} has the property that $\hat{A}\hat{A}^\dagger = \hat{A}^\dagger\hat{A} = \hat{I}$.

$$\begin{aligned}
&= i\hbar \sum_m \sum_n e^{i[\sigma_n(t) - \sigma_m(t)]} (|\dot{n}(t)\rangle \langle n(0)|m(0)\rangle \langle m(t)| + i\dot{\sigma}_n(t) |n(t)\rangle \langle n(0)|m(0)\rangle \langle m(t)|) = \\
&= i\hbar \sum_n (|\dot{n}(t)\rangle \langle n(t)| + i\dot{\sigma}_n(t) |n(t)\rangle \langle n(t)|).
\end{aligned}$$

Deriving $\sigma_n(t)$,

$$\begin{aligned}
\hat{H}(t) &= i\hbar \sum_n \left[|\dot{n}(t)\rangle \langle n(t)| + i \left(-\frac{1}{\hbar} E_n(t) + i \langle n(t)|\dot{n}(t)\rangle \right) |n(t)\rangle \langle n(t)| \right], \\
\rightarrow \hat{H}(t) &= \sum_n [i\hbar |\dot{n}(t)\rangle \langle n(t)| + E_n |n(t)\rangle \langle n(t)| - i\hbar \langle n(t)|\dot{n}(t)\rangle |n(t)\rangle \langle n(t)|]. \quad (3.18)
\end{aligned}$$

From equation (3.12), the second term in equation (3.18) is simply $\hat{H}_0(t)$. Hence,

$$\hat{H}(t) = \hat{H}_0(t) + \hat{H}_{CD}(t), \quad (3.19)$$

with

$$\hat{H}_{CD}(t) = i\hbar \sum_n [|\dot{n}(t)\rangle \langle n(t)| - \langle n(t)|\dot{n}(t)\rangle |n(t)\rangle \langle n(t)|]. \quad (3.20)$$

The determination of the counterdiabatic Hamiltonian in equation (3.20) requires the knowledge of the instantaneous eigenstates of the reference Hamiltonian, which is not usually an easy task to realize. In spite of this, the counterdiabatic protocol has been applied in a wide variety of systems with considerable success, from promoting population transfer in atomic and molecular systems (CHEN et al., 2010; CHEN; MUGA, 2012) to the generation of large entangled states (CHEN et al., 2021) and the realisation of quantum state transfer in long spin chains (ZHOU et al., 2019).

To finish with an example, we show in figure 2 the population inversion between two fundamental energy levels $|1\rangle$ and $|3\rangle$, assisted by a higher energy level $|2\rangle$, in a three-level atomic model, performed by two different protocols. The details of how this process can happen will be presented in chapter 4. In the first image, we observe the execution via a reference protocol, called Stimulated Raman Adiabatic Passage, or *STIRAP*, in a time much smaller than that required to be adiabatic, so that population inversion is not achieved. In the second image, the second protocol, which is a counterdiabatic acceleration of the STIRAP, is applied with the same amount of time, and the inversion is complete (LI; CHEN, 2016).

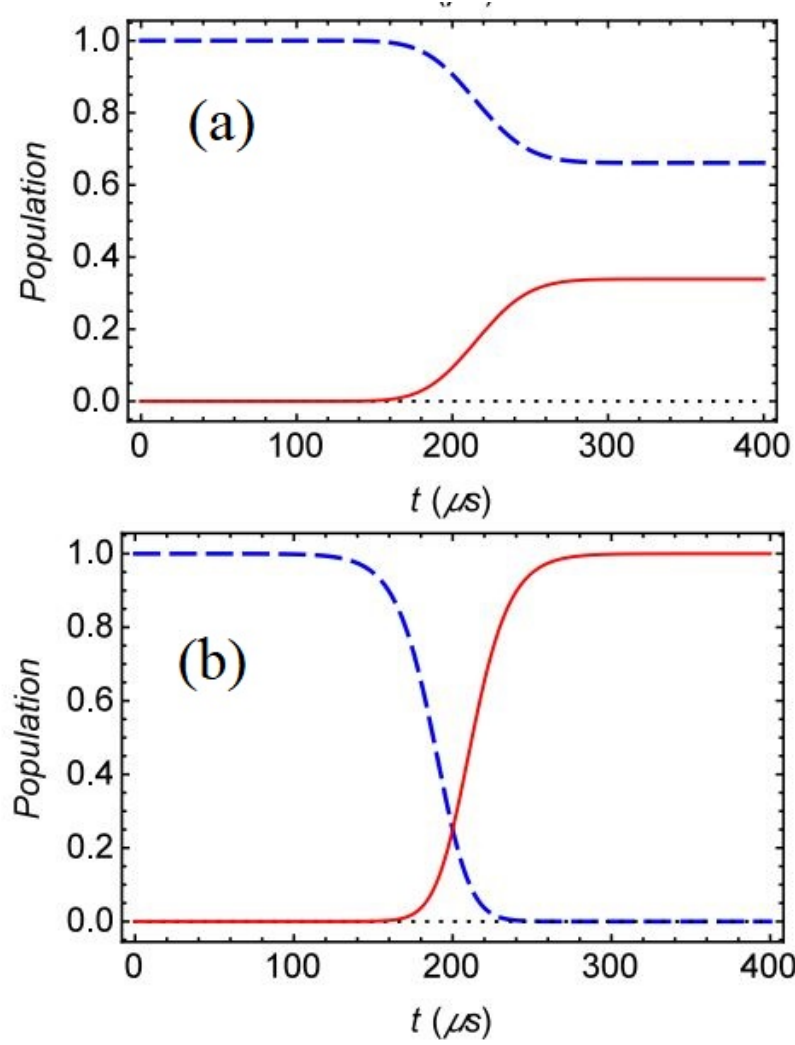


Figure 2 – Populations of the levels $|1\rangle$ (blue), $|2\rangle$ (black) and $|3\rangle$ (red) of an atomic system during a process of population transfer through the (a) reference protocol in non-adiabatic time, and (b) counterdiabatic protocol. Extracted from (LI; CHEN, 2016).

3.4 Time-rescaling as a STA

The time-rescaling protocol (TR protocol), proposed by B. L. Bernardo in 2020, is a considerably simple method to perform a STA through the modification of the time parameter t , from which a new Hamiltonian is determined. This is the chosen STA protocol to be used in subsequent parts of this work.

It is known that a closed quantum system evolves in time through a unitary time-evolution operator $\hat{U}(t_f, t_0)$, which is a solution to the Schrödinger equation,

$$i\hbar \frac{\partial}{\partial t} \hat{\mathcal{U}}(t_f, t_0) = \hat{H}(t) \hat{\mathcal{U}}(t_f, t_0). \quad (3.21)$$

Here, $\hat{H}(t)$ is the reference, time-dependent Hamiltonian that generates the original time evolution of the system. This equation (3.21) can be solved to yield

$$\hat{\mathcal{U}}(t_f) = \hat{\mathcal{T}} \exp \left[-\frac{i}{\hbar} \int_0^{t_f} \hat{H}(t) dt \right], \quad (3.22)$$

where we set $t_0 = 0$ for convenience.

We now develop the time-rescaling method. Its essence is to redefine (or rescale) the time variable as a function of a new variable τ , so that $t = f(\tau)$. By applying this to equation (3.22), we obtain

$$\hat{\mathcal{U}}[f^{-1}(t_f)] = \hat{\mathcal{T}} \exp \left[-\frac{i}{\hbar} \int_{f^{-1}(0)}^{f^{-1}(t_f)} \hat{H}[f(\tau)] \dot{f}(\tau) d\tau \right],$$

or

$$\hat{\mathcal{U}}(t_f) = \hat{\mathcal{T}} \exp \left[-\frac{i}{\hbar} \int_{f^{-1}(0)}^{f^{-1}(t_f)} \hat{\mathcal{H}}(\tau) d\tau \right], \quad (3.23)$$

and the new Hamiltonian, $\hat{\mathcal{H}}(\tau)$, called *TR Hamiltonian*, is given by

$$\hat{\mathcal{H}}(\tau) = \hat{H}[f(\tau)] \dot{f}(\tau). \quad (3.24)$$

It is important to observe that both equations (3.22) and (3.23) represent the same evolution. Hence, a system at state $|\psi(0)\rangle$ will end up at state $|\psi(t_f)\rangle$ through both the reference and TR protocols. However, while the reference evolution will be generated by the Hamiltonian $\hat{H}(t)$, and takes a time $\Delta t = t_f$ to occur, the TR evolution is generated by the $\hat{\mathcal{H}}(\tau)$ Hamiltonian, which takes a time $\Delta \tau = f^{-1}(t_f) - f^{-1}(0)$ to occur. If the reference protocol is adiabatic and $\Delta \tau < \Delta t$, then the TR protocol acts as a shortcut to adiabaticity.

To guarantee that the TR protocol indeed acts as a STA, we impose certain conditions: (i) $f^{-1}(0) = 0$ and $f^{-1}(t_f) < t_f$, and (ii) $\hat{\mathcal{H}}(\tau) = \hat{H}(t)$ at the initial and final times. The first condition ensures that the new protocol is faster than the reference one. The second ensures that the initial and final Hamiltonian of the reference and TR dynamics are identical. This is important to guarantee that the system will be in a stable (stationary) state of the Hamiltonian at the beginning and in the end of the TR process,

as it is in the reference one. The first condition is easy to satisfy; the second is realizable by choosing a rescaling function $f(\tau)$ such that $\dot{f}[f^{-1}(0)] = \dot{f}[f^{-1}(t_f)] = 1$. The possibility to use the TR protocol as a STA becomes, then, a matter of choosing a suitable rescaling function.

In principle, there might be many different functions satisfying these conditions. Here, we choose to use the following one: (BERNARDO, 2020)

$$f(\tau) = a\tau - \frac{t_f}{2\pi a}(a-1)\sin\left(\frac{2\pi a}{t_f}\tau\right), \quad (3.25)$$

where a is a real constant. From equation (3.25), we observe that $f^{-1}(0) = 0$ and $f^{-1}(t_f) = t_f/a$. If $a > 1$, the TR protocol takes less time than the reference one, and becomes an STA protocol (satisfying the first condition). For this reason, a was named *contraction parameter*. From equation (3.25) we also obtain,

$$f'(\tau) = a - (a-1)\cos\left(\frac{2\pi a}{t_f}\tau\right), \quad (3.26)$$

from which we obtain that $f'(0) = f'(t_f/a) = 1$. Hence, the second condition is also satisfied.

In practice, the TR protocol works by modifying the original Hamiltonian in terms of the rescaling function, and then performing the process between $t = 0$ and $t = t_f/a$. Depending on the system of interest, this modification may include introducing changes such as time-dependent magnetic fields or extra laser pulses. The protocol drives the system to the same final state generated by the reference (adiabatic) process, but at a shorter time duration (if $a > 1$). During its application, though, no adiabatic properties are conserved, in principle. In mathematical terms, the protocol is quite simple, as well as state-independent (the initial state does not have to be an eigenstate of the Hamiltonian, and no knowledge of the instantaneous eigenstates and eigenvalues of the reference Hamiltonian are required). It has also a wider range of applications - we supposed a situation where the reference protocol is adiabatic, but such condition is not required: any reference protocol can be accelerated through the TR method.

The time-rescaling protocol has already been applied in certain problems such as the parametric oscillator, the transport of a particle in a trap and the population inversion in two-level atomic systems (BERNARDO, 2020; ANDRADE; FRANÇA; BERNARDO, 2022) with considerable success. Application of the method has also achieved success in quantum relativistic problems, such as the dynamics of Weyl semimetals (ROYCHOWDBURY; DEFFNER, 2021).

4 STIRAP Protocol

In this chapter we discuss the STIRAP method to perform controlled population transfer in three-level systems. We begin with a discussion about Raman scattering, a phenomenon whose elements are used in performing the STIRAP. Then, we give a general view of the protocol, followed by two subsections of mathematical details. The following section presents some particular characteristics or conditions of the STIRAP protocol. The final subsection explains how the protocol is performed in practice.

4.1 Raman Scattering

Light scattering is a group of phenomena associated to the interactions of light with a given medium, or the individual interactions (normally treated as collisions) of photons with other particles. The first type of light scattering to be described was the Raleigh scattering, discovered in the nineteenth century by Lord Rayleigh ([STRUTT, 1871](#)). At the beginning of the twentieth century, Mie scattering was discovered by Gustav Mie ([MIE, 1908](#)). A common characteristic of these two is that they are both elastic: the photon conserves its energy, so that only changes in phase result from the interaction (Rayleigh scattering happens when light interacts with particles much smaller than its wavelength, while Mie scattering when the interaction is with particles of about the same size as the wavelength). Then, in 1928, C. V. Raman and his coworker, K. S. Krishnan, reported the discovery of a new type of scattering of light in molecules, which is inelastic. It was later named “Raman scattering” ([RAMAN, 1928](#)).

Raman scattering can be understood through a semi-classical model as follows ([KERESZTURY, 2002](#)): radiation from an exciting source (named pump) is absorbed by a molecule at a given initial state, which is then excited to a virtual energy level. It then spontaneously emits, transitioning to a lower, real level. If the final level is higher than the initial one, part of the energy of the incident radiation was captured in the form of vibrational energy by the molecule; this is the Stokes Raman scattering, and the exiting radiation is named likewise, Stokes. If the final level is lower than the initial one, vibrational energy of the molecule was lost to the exiting radiation; this is called “anti-Stokes Raman scattering”, the exiting radiation being equally named. Mathematically,

$$\nu_{s/as} = \nu_p \mp \frac{\Delta E_{vib}}{h}, \quad (4.1)$$

with $\nu_{s/as}$ being the Stokes/anti-Stokes radiation frequency, ν_p the pump frequency, ΔE_{vib} the energy difference between the real vibrational energy levels involved and h , the Planck constant. The process can be pictured as in figure 3. The collection of Stokes and anti-Stokes spectral lines, pertaining to the various transitions between vibrational levels are called *Raman spectrum*.

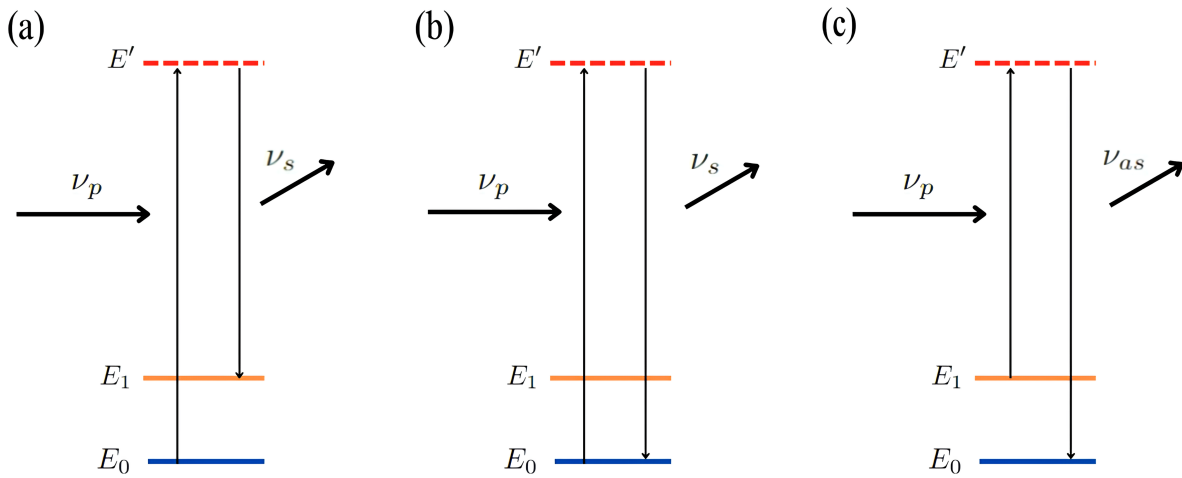


Figure 3 – Semi-classical model of interaction between a molecular system and an external (pump) radiation field of frequency ν_p . (a) Stokes Raman scattering: energy is absorbed from the pump and, upon emission, part is kept in form of vibrational energy, so that $\nu_s < \nu_p$. (b) Rayleigh (elastic) scattering: no energy is retained by the molecule, $\nu_s = \nu_p$. (c) Anti-Stokes Raman scattering: energy is absorbed from the pump and, upon emission, part of the original vibrational energy is lost to the exiting radiation ($\nu_{as} > \nu_p$).

It is important to observe that only about 0.0001% of the incident radiation experiences Raman scattering; hence, the observation of a distinct spectrum requires the use of strong radiation sources, normally achieved by high-quality lasers (GARDINER; GRAVES, 1989). Also, the intensity rate between Stokes and anti-Stokes Raman scattering will depend on the populations of the different vibrational levels, which in turn depend on the temperature of the sample. Since (except at an infinite temperature), lower levels are more populated, we have that the ratio of the intensities normally obeys $I_{as}/I_s < 1$.

Raman scattering has a wide range of applications, specially in the characterization of the vibrational and rotational properties of molecules and solids. It is one of the most useful phenomena within molecular spectroscopy (MCCREERY, 2000).

4.2 General idea of the STIRAP Protocol

The spontaneous emission resulting in Raman scattering can create an entire spectrum, due to the many possible realisable transitions. If the decay is stimulated, however, it is possible, in principle, to control the decay of the molecule into a desired state. Further yet, such stimulated passage could allow population transfers between two states of any kind of three-level system. This is the basis of the STIRAP protocol, to be presented in this section.

STIRAP, *Stimulated Raman Adiabatic Passage*, is a technique developed from 1989 onward by K. Bergmann and others, to perform adiabatic population transfer in three-level systems (KUKLINSKI et al., 1989; VITANOV et al., 2001; DJOTYAN et al., 2000; SHORE, 2017). Calling these states $|1\rangle$, $|2\rangle$ and $|3\rangle$, the idea is to move the population from $|1\rangle \rightarrow |3\rangle$, with the help of state $|2\rangle$, but having no significant population in this second level at any moment of the process. Although it was, at first, mainly focused in transfers between vibrational states of molecules, it soon became applicable in a wide variety of physical systems (VITANOV et al., 2017; BERGMANN et al., 2017).

Our focus here will be the case of a three-level Λ atomic system - meaning that both states $|1\rangle$ and $|3\rangle$ have lower energy than $|2\rangle$. Their representation is given in figure 4. Just as in the case of the Raman scattering, two radiation fields will be involved: a pump field, to excite the atomic system from state $|1\rangle$ to $|2\rangle$, and a Stokes field, to stimulate decay from $|2\rangle$ to $|3\rangle$. The details on how these fields promote transitions in the atomic system were discussed in section 2.2 of the previous chapter.

It is important to point out that the arrangement is such that the pump and Stokes fields are only significant on their effect over the desired energy levels: $|1\rangle \rightarrow |2\rangle$ and $|2\rangle \rightarrow |3\rangle$, respectively. Hence, any direct transitions between $|1\rangle$ and $|3\rangle$, as well as the existence of probability loss (transitions to levels other than the three-level approximation), can be considered null.

4.3 Rotating Wave Approximation Hamiltonian

Before discussing the STIRAP protocol in itself, it is important to write the system's Hamiltonian in a convenient manner. Consider the Schrödinger equation applied to the

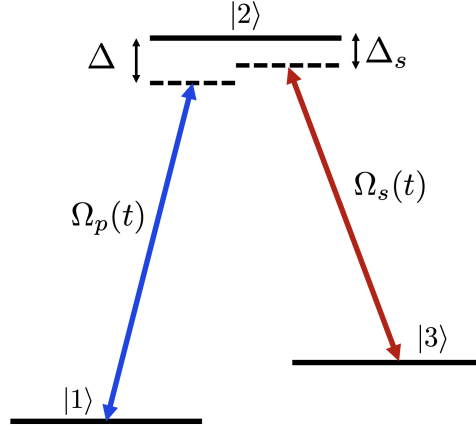


Figure 4 – Conceptual schematics of a Λ three-level atomic system, under the influence of external Stokes and pump laser pulses of respective Rabi frequencies $\Omega_s(t)$ and $\Omega_p(t)$. The solid lines represent the undisturbed atomic energy levels, while dashed lines represent the virtual levels. The detuning of the Stokes and the pump fields with respect to the real atomic levels are given by Δ_s and Δ .

three-level atomic system just discussed. It can be written from equation (2.7), that

$$i\hbar \begin{pmatrix} \dot{c}_1 \\ \dot{c}_2 \\ \dot{c}_3 \end{pmatrix} = \begin{pmatrix} E_1 - \hbar\dot{\xi}_1(t) & V_{12}e^{-i(\xi_2-\xi_1)} & 0 \\ V_{12}^*e^{i(\xi_2-\xi_1)} & E_2 - \hbar\dot{\xi}_2(t) & V_{23}e^{-i(\xi_3-\xi_2)} \\ 0 & V_{23}^*e^{i(\xi_3-\xi_2)} & E_3 - \hbar\dot{\xi}_3(t) \end{pmatrix} \begin{pmatrix} c_1 \\ c_2 \\ c_3 \end{pmatrix}, \quad (4.2)$$

in the $\{|1\rangle, |2\rangle, |3\rangle\}$ basis. Here, the E_i 's are the energies of the atomic levels, ξ_i 's are arbitrary phases to be conveniently chosen and, V_{ij} the elements of the matrix of the Hamiltonian of interaction ($i, j = 1, 2, 3$). The terms $V_{ii} = 0$, from equation (2.18).

The external electric field acting on the system can be written as,

$$\mathbf{E}(t) = \frac{1}{2} \left[\hat{\epsilon}_p \mathcal{E}_p(t) (e^{-i\omega_p t} + e^{i\omega_p t}) + \hat{\epsilon}_s \mathcal{E}_s(t) (e^{-i\omega_s t} + e^{i\omega_s t}) \right], \quad (4.3)$$

with $\hat{\epsilon}_i$ as the polarization unit-vectors, \mathcal{E}_i the amplitudes of the fields, and ω_i the frequencies ($i = p, s$). From the last chapter, section 2.2, the elements of the Hamiltonian of interaction are given by $V_{ij} = -\langle i | \mathbf{d} \cdot \mathbf{E}(t) | j \rangle$, and from the definition of the Rabi frequencies in equation (2.19),

$$\Omega_p(t) = -\frac{e\mathcal{E}_p(t)}{\hbar} \langle 1 | \mathbf{r} \cdot \hat{\epsilon} | 2 \rangle, \quad (4.4a)$$

$$\Omega_s(t) = -\frac{e\mathcal{E}_s(t)}{\hbar} \langle 2 | \mathbf{r} \cdot \hat{\epsilon} | 3 \rangle, \quad (4.4b)$$

we find that,

$$V_{13} = V_{31} = 0, \quad (4.5a)$$

$$V_{12} = V_{21} = \frac{\hbar\Omega_p}{2} (e^{-i\omega_p t} + e^{i\omega_p t}), \quad (4.5b)$$

$$V_{13} = V_{31} = \frac{\hbar\Omega_s}{2} (e^{-i\omega_s t} + e^{i\omega_s t}). \quad (4.5c)$$

From now on, the explicit time dependence of the Rabi frequencies (and other time dependent functions) might be omitted in the future, for economy.

Now, the phases ξ_i are chosen. For a Λ system, an appropriate choice (KEYLON; DEPOALA, 2015; ASSÉMAT, 2013) would be

$$\xi_2 - \xi_1 = \omega_p t \rightarrow \dot{\xi}_2 = \dot{\xi}_1 + \omega_p, \quad (4.6a)$$

$$\xi_3 - \xi_2 = -\omega_s t \rightarrow \dot{\xi}_3 = \dot{\xi}_2 - \omega_s. \quad (4.6b)$$

Applying equations (4.5a), (4.5b), (4.5c), (4.6a) and (4.6b) into equation (4.2), we obtain

$$\hat{H} = \begin{pmatrix} E_1 - \hbar\dot{\xi}_1(t) & \frac{\hbar\Omega_p}{2} (e^{-i\omega_p t} + e^{i\omega_p t}) e^{-i\omega_p t} & 0 \\ \frac{\hbar\Omega_p}{2} (e^{-i\omega_p t} + e^{i\omega_p t}) e^{i\omega_p t} & E_2 - \hbar\dot{\xi}_1 - \hbar\omega_p & \frac{\hbar\Omega_s}{2} (e^{-i\omega_s t} + e^{i\omega_s t}) e^{i\omega_s t} \\ 0 & \frac{\hbar\Omega_s}{2} (e^{-i\omega_s t} + e^{i\omega_s t}) e^{-i\omega_s t} & E_3 - \hbar\dot{\xi}_1 - \hbar\omega_p + \hbar\omega_s \end{pmatrix}. \quad (4.7)$$

Simplifying the entries of the above matrix and choosing $\dot{\xi}_1 = E_1/\hbar$ for convenience, we can write

$$\hat{H} = \begin{pmatrix} 0 & \frac{\hbar\Omega_p}{2} (e^{-2i\omega_p t} + 1) & 0 \\ \frac{\hbar\Omega_p}{2} (1 + e^{2i\omega_p t}) & E_2 - E_1 - \hbar\omega_p & \frac{\hbar\Omega_s}{2} (1 + e^{2i\omega_s t}) \\ 0 & \frac{\hbar\Omega_s}{2} (e^{-2i\omega_s t} + 1) & E_3 - E_1 - \hbar\omega_p + \hbar\omega_s \end{pmatrix}. \quad (4.8)$$

Below we point out some important definitions:

1. The one-photon detuning is defined as the difference between the Bohr frequency, $\omega_{ij} = (E_i - E_j)/\hbar$, and the frequency of the external radiation field. In our case, we have two one-photon detunings of importance,

$$\Delta = \omega_{21} - \omega_p, \quad (4.9a)$$

$$\Delta_s = \omega_{23} - \omega_s. \quad (4.9b)$$

2. The two-photon detuning is defined as the difference between the detunings created by the two radiation fields on the respective energy levels, here given by

$$\delta = \Delta - \Delta_s. \quad (4.10)$$

By adding and subtracting E_2 in the element (3, 3) of equation (4.8), we obtain precisely equation (4.10). We also apply the definitions of equations (4.9a) and (4.9b) and put the $\hbar/2$ term in evidence, to obtain,

$$\hat{H} = \frac{\hbar}{2} \begin{pmatrix} 0 & \Omega_p (e^{-2i\omega_p t} + 1) & 0 \\ \Omega_p (1 + e^{2i\omega_p t}) & 2\Delta & \Omega_s (1 + e^{2i\omega_s t}) \\ 0 & \Omega_s (e^{-2i\omega_s t} + 1) & 2\delta \end{pmatrix}. \quad (4.11)$$

Finally, we apply the rotating wave approximation (RWA), which consists in eliminating terms that rotate “fast” in the chosen frame of reference. In our case, the particular frame is determined by the phase factors chosen within the interaction picture. Observe in eq. (4.11) that these phase factors allow to re-write the electric fields of the external radiation in terms of a stationary term (called rotating term), plus a term rotating with frequency $2\omega_{p,s}$ (counter-rotating term). Now, the dynamics of the atomic system is given by the time evolution operator (eq. (3.22)), which to be obtained requires to integrate this Hamiltonian. The integration of a phase factor like $e^{in\omega t}$ yields,

$$\int_0^{t_f} e^{in\omega t} dt = \frac{1}{in\omega} (e^{in\omega t_f} - 1), \quad (4.12)$$

which is $\ll 1$ if the product $n\omega$ is considerably large and the field intensities (and as a consequence, the Rabi frequencies) are sufficiently low. For the characteristics of our problem, this approximation is applicable (FUJII, 2017). Hence, we eliminate the terms $e^{2i\omega_{p,s}t}$ from eq. (4.11), which becomes,

$$\hat{H} = \frac{\hbar}{2} \begin{pmatrix} 0 & \Omega_p & 0 \\ \Omega & 2\Delta_p & \Omega_s \\ 0 & \Omega_s & 2\delta \end{pmatrix}, \quad (4.13)$$

4.4 Eigenvalues and Eigenstates

From equation (4.13), we proceed by imposing a special condition to perform the STIRAP protocol: the two-photon detuning must be zero ($\delta = 0$). The reason for that will be justified in the next section. Hence, the Hamiltonian becomes

$$\hat{H} = \frac{\hbar}{2} \begin{pmatrix} 0 & \Omega_p & 0 \\ \Omega_p & 2\Delta & \Omega_s \\ 0 & \Omega_s & 0 \end{pmatrix}, \quad (4.14)$$

The energy eigenvalues can be calculated through the characteristic equation,

$$\det(\hat{H} - E_n \hat{I}) = 0, \quad (4.15)$$

yielding,

$$\det \left[\frac{\hbar}{2} \begin{pmatrix} -E_n & \Omega_p & 0 \\ \Omega_p & 2\Delta - E_n & \Omega_s \\ 0 & \Omega_s & -E_n \end{pmatrix} \right] = 0,$$

which implies,

$$E_n^2(2\Delta - E_n) + (\Omega_p^2 + \Omega_s^2)E_n = 0.$$

This is satisfied for

$$E_n = 0,$$

$$E_n^2 - 2\Delta E_n - \Omega^2 = 0,$$

with $\Omega = \sqrt{\Omega_p^2 + \Omega_s^2}$. We solve the second (quadratic) equation to obtain the roots $E_n(t) = \frac{\hbar}{2} (\Delta \pm \sqrt{\Delta^2 + \Omega^2})$. Hence, the eigenvalues this Hamiltonian are,

$$E_+(t) = \frac{\hbar}{2} \left(\Delta + \sqrt{\Delta^2 + \Omega^2} \right), \quad (4.16a)$$

$$E_0(t) = 0, \quad (4.16b)$$

$$E_-(t) = \frac{\hbar}{2} \left(\Delta - \sqrt{\Delta^2 + \Omega^2} \right). \quad (4.16c)$$

To continue the analysis, we introduce two “mixing angles”¹ θ and ϕ , defined as $\tan \theta(t) = \Omega_p(t)/\Omega_s(t)$ and $\tan 2\phi(t) = \Omega(t)/\Delta$ (BERGMANN; VITANOV; SHORE, 2015), and then transform equations (4.16a), (4.16b) and (4.16c). First,

$$\begin{aligned} \Delta \pm \sqrt{\Delta^2 + \Omega^2} &= \Omega \left[\frac{\Delta}{\Omega} \pm \sqrt{\left(\frac{\Delta}{\Omega} \right)^2 + 1} \right] = \\ &= \Omega \left[\frac{1}{\tan(2\phi)} \pm \sqrt{\left(\frac{1}{\tan(2\phi)} \right)^2 + 1} \right] = \Omega \left[\frac{\cos(2\phi)}{\sin(2\phi)} \pm \frac{1}{\sin(2\phi)} \right] = \\ &= \Omega \left[\frac{\cos(2\phi) \pm 1}{\sin(2\phi)} \right]. \end{aligned} \quad (4.17)$$

From now on, we may omit the explicit time dependency “(t)” of the mixing angles, eigenenergies and eigenstates, for economy. Now, $\sin 2\phi = 2 \sin \phi \cos \phi$, and for $E_{(+)}$, we use the identity $\cos 2\phi = 2 \cos^2 \phi - 1$ in equation (4.17), and for $E_{(-)}$, the identity $\cos 2\phi = 1 - 2 \sin^2(\phi)$, to obtain,

$$E_+ = \frac{\hbar\Omega}{2} \cot \phi, \quad (4.18a)$$

$$E_0 = 0, \quad (4.18b)$$

$$E_- = -\frac{\hbar\Omega}{2} \tan \phi. \quad (4.18c)$$

¹ The term ‘mixing’ angles comes from the fact that they are the angles, in the respective Hilbert space, between the orthogonal eigenvectors of the undisturbed H Hamiltonian. Hence, they are used to construct states which are a ‘mix’ of those.

Having the eigenenergies, it is possible to obtain the eigenstates through the eigenvalue equation (3.1). Writting $|n(t)\rangle = c_1 |1\rangle + c_2 |2\rangle + c_3 |3\rangle$, with c_1, c_2, c_3 being complex numbers, we obtain:

- For E_0 ,

$$\frac{\hbar}{2} \begin{pmatrix} 0 & \Omega_p & 0 \\ \Omega_p & 2\Delta & \Omega_s \\ 0 & \Omega_s & 0 \end{pmatrix} \begin{pmatrix} c_1 \\ c_2 \\ c_3 \end{pmatrix} = 0 \rightarrow \begin{aligned} \Omega_p c_2 &= 0, \\ \Omega_p c_1 + 2\Delta c_2 + \Omega_s c_3 &= 0, \\ \Omega_s c_2 &= 0, \end{aligned}$$

from which $c_2 = 0$ and $c_3 = -(\Omega_p/\Omega_s)c_1 = -\tan(\theta)c_1$. The amplitude c_1 can be determined through the normalization condition,

$$|c_1|^2 + |c_2|^2 + |c_3|^2 = 1,$$

$$(\tan^2 \theta + 1)|c_1|^2 = 1,$$

$$|c_1|^2 = \cos^2 \theta,$$

$$c_1 = \cos \theta,$$

where we considered c_1 as real, for convenience. Hence,

$$|n_0(t)\rangle = \cos \theta(t) |1\rangle - \sin \theta(t) |3\rangle. \quad (4.19)$$

- For E_+ ,

$$\frac{\hbar}{2} \begin{pmatrix} 0 & \Omega_p & 0 \\ \Omega_p & 2\Delta & \Omega_s \\ 0 & \Omega_s & 0 \end{pmatrix} \begin{pmatrix} c_1 \\ c_2 \\ c_3 \end{pmatrix} = \frac{\hbar\Omega}{2} \cot \phi \begin{pmatrix} c_1 \\ c_2 \\ c_3 \end{pmatrix} \rightarrow \begin{aligned} \Omega_p c_2 &= \Omega \cot \phi c_1, \\ \Omega_p c_1 + 2\Delta c_2 + \Omega_s c_3 &= \Omega \cot \phi c_2, \\ \Omega_s c_2 &= \Omega \cot \phi c_3. \end{aligned}$$

In the above relations we have that $c_1 = (\Omega_p/\Omega) \tan \phi c_2 = \sin(\theta) \tan \phi c_2$ and $c_3 = (\Omega_s/\Omega) \tan \phi c_2 = \cos \theta \tan \phi c_2$. The amplitude c_2 can be determined through the normalization condition,

$$|c_1|^2 + |c_2|^2 + |c_3|^2 = 1,$$

$$[\sin^2 \theta \tan^2 \phi + \cos^2 \theta \tan^2 \phi + 1]|c_2|^2 = 1,$$

$$[\tan^2 \phi + 1]|c_1|^2 = 1,$$

$$|c_2|^2 = \cos^2 \phi,$$

$$c_2 = \cos \phi,$$

where we considered c_2 as real, for convenience. Hence,

$$|n_+(t)\rangle = \sin \theta(t) \sin \phi(t) |1\rangle + \cos \phi(t) |2\rangle + \cos \theta(t) \sin \phi(t) |3\rangle. \quad (4.20)$$

- For E_- ,

$$\frac{\hbar}{2} \begin{pmatrix} 0 & \Omega_p & 0 \\ \Omega_p & 2\Delta & \Omega_s \\ 0 & \Omega_s & 0 \end{pmatrix} \begin{pmatrix} c_1 \\ c_2 \\ c_3 \end{pmatrix} = -\frac{\hbar\Omega}{2} \tan \phi \begin{pmatrix} c_1 \\ c_2 \\ c_3 \end{pmatrix} \rightarrow \begin{aligned} \Omega_p c_2 &= -\Omega \tan \phi c_1, \\ \Omega_p c_1 + 2\Delta c_2 + \Omega_s c_3 &= -\Omega \tan \phi c_2, \\ \Omega_s c_2 &= -\Omega \tan \phi c_3, \end{aligned}$$

from which $c_1 = -\sin \theta \cot \phi c_2$ and $c_3 = -\cos \theta \cot \phi c_2$. Again, the amplitude c_2 can be determined through the normalisation condition,

$$|c_1|^2 + |c_2|^2 + |c_3|^2 = 1,$$

$$[\sin^2 \theta \cot^2 \phi + \cos^2 \theta \cot^2 \phi + 1]|c_2|^2 = 1,$$

$$[\cot^2 \phi + 1]|c_1|^2 = 1,$$

$$|c_2|^2 = \sin^2 \phi,$$

$$c_2 = \sin \phi,$$

where, again, we considered c_2 as real, for convenience. Hence²,

$$|n_-(t)\rangle = \sin \theta(t) \cos \phi(t) |1\rangle - \sin \phi(t) |2\rangle + \cos \theta(t) \cos \phi(t) |3\rangle. \quad (4.21)$$

² An overall negative sign was applied for convenience, without changing the result, since global phases have no physical importance.

4.5 Special Conditions for the STIRAP

In this subsection we discuss some special conditions necessary to perform the STIRAP protocol. The first condition was already imposed in the previous subsection: there must not exist two-photon detuning. The reason for that has now become clear - one of the eigenstates of the Hamiltonian under the $\delta = 0$ condition, $|n_0(t)\rangle$, is the so called “dark state” (DAVIS; METCALF; PHILLIPS, 1979; DOERY et al., 1995). If the system remains in this state while it evolves, the population transfer can occur from $|1\rangle$ to $|3\rangle$, without reference to state $|2\rangle$. This prevents probability loss from that state, through spontaneous emission.

The second condition is not necessary, but has been historically accepted for convenience (VITANOV et al., 2001; SHORE, 2017; VITANOV et al., 2017): the one-photon detuning, Δ , is set as a constant value. The third condition imposes the adiabaticity of the protocol, and is divided into two parts:

1. *Local adiabatic condition.* The adiabatic theorem discussed in section 3.1 shows that the system remains in a given eigenstate of the Hamiltonian (apart from a gain of phase), if the condition in equation (3.9) is satisfied,

$$\left| \frac{\langle m(t) | \dot{H} | n(t) \rangle}{E_n - E_m} \right| \ll \frac{E_m}{\hbar}. \quad (4.22)$$

This leads to a local adiabatic condition. Since we decided to study the STIRAP, the the system is originally prepared in the $|n_0(t)\rangle$ eigenstate (as we shall see in the next section), we evaluate the adiabatic theorem effect in the possible transitions between $|n_0(t)\rangle \leftrightarrow |n_+(t)\rangle$ and $|n_0(t)\rangle \leftrightarrow |n_-(t)\rangle$. First, we obtain the time-derivative of the Hamiltonian given in equation (4.13),

$$\dot{H} = \frac{\hbar}{2} \begin{pmatrix} 0 & \dot{\Omega}_p & 0 \\ \dot{\Omega}_p & 0 & \dot{\Omega}_s \\ 0 & \dot{\Omega}_s & 0 \end{pmatrix}, \quad (4.23)$$

and by applying equations (4.23), (4.16a), (4.16b), (4.16c), (4.19), (4.20) and (4.21) in equation (4.22), we find that

$$\left| \frac{\langle n_+(t) | \dot{H} | n_0(t) \rangle}{E_+ - E_0} \right| = \left| \frac{\frac{\hbar}{2} \cos \phi (\cos \theta \dot{\Omega}_p - \sin \theta \dot{\Omega}_s)}{\frac{\hbar}{2} \Omega \cot \phi} \right| \ll \frac{1}{2} \Omega \cot \phi, \quad (4.24a)$$

and

$$\left| \frac{\langle n_-(t) | \dot{H} | n_0(t) \rangle}{E_- - E_0} \right| = \left| \frac{\frac{\hbar}{2} \cos \phi (\cos \theta \dot{\Omega}_p - \sin \theta \dot{\Omega}_s)}{\frac{\hbar}{2} \Omega \tan \phi} \right| \ll \frac{1}{2} \Omega \tan \phi. \quad (4.24b)$$

Now, from the definition of the mixing angle $\theta(t)$,

$$\frac{d}{dt} \tan \theta = \frac{d}{dt} \left(\frac{\Omega_p}{\Omega_s} \right),$$

$$\frac{1}{\cos^2 \theta} \dot{\theta} = \frac{\Omega^2}{\Omega_s^2} \dot{\theta}(t) = \frac{\dot{\Omega}_p \Omega_s - \dot{\Omega}_s \Omega_p}{\Omega_s^2},$$

and since $\sin \theta = \Omega_p / \Omega$ and $\cos \theta = \Omega_s / \Omega$, we have that

$$\dot{\theta}(t) = \frac{\dot{\Omega}_p \Omega_s - \dot{\Omega}_s \Omega_p}{\Omega^2}. \quad (4.25)$$

By substitution of equation (4.25) into equations (4.24a) and (4.24b) and organizing them, we obtain,

$$\left| \left(\frac{\sin \phi^2}{\cos \phi} \right) \dot{\theta} \right| \ll \frac{1}{2} \Omega, \quad (4.26a)$$

and

$$\left| \left(\frac{\cos \phi^2}{\sin \phi} \right) \dot{\theta} \right| \ll \frac{1}{2} \Omega. \quad (4.26b)$$

It is important to evaluate two regimes of particular importance: (i) the resonance ($\Delta = 0$) and (ii) at large detunings ($\Delta \gg \Omega$). Since $\phi(t)$ is defined by $\tan 2\phi(t) = \Omega / \Delta$, for the first case we have that $\tan 2\phi \rightarrow \infty$, so that $2\phi = \frac{\pi}{2}$, and $\phi = \frac{\pi}{4}$, which results in $\sin^2 \phi = 1/2$ and $\cos \phi = \sqrt{2}/2$. These values turn both condition (4.26a) and condition (4.26b) into the same expression:

$$|\dot{\theta}| \ll \Omega(t). \quad (4.27)$$

For the second regime, $\tan 2\phi \rightarrow 0$, allowing for the approximations $\tan 2\phi \approx \sin 2\phi \approx 2\phi$ and $\cos 2\phi = 2\cos^2 \phi - 1 \approx 1$, so that $\cos \phi \approx 1$, and the conditions in equations (4.26a) and (4.26b) become:

$$\left| \left(\frac{\Omega^2}{4\Delta^2} \right) \dot{\theta} \right| \ll \frac{1}{2}\Omega, \quad (4.28a)$$

and

$$\left| \left(\frac{2\Delta}{\Omega} \right) \dot{\theta} \right| \ll \frac{1}{2}\Omega. \quad (4.28b)$$

The second condition becomes more restrictive, so we continue only with it. Since both Δ and Ω are positive, we obtain that

$$\Delta |\dot{\theta}| \ll \frac{1}{4}\Omega^2. \quad (4.29)$$

Equations (4.27) and (4.29) are, in their respective regimes, the “local conditions for adiabaticity”, since they must be satisfied at all times.

It is common in the literature to consider a “worst case scenario” (SHORE, 2017; VITANOV et al., 2001): if the pulses have the same peak value, Ω_0 , and if they are both sufficiently smooth, then $\Omega(t)$ has an upper bound, $\Omega(t) \leq \sqrt{2}\Omega_0$. The worst case scenario, then, imposes the local adiabatic conditions in the limit,

$$|\dot{\theta}| \ll \Omega_0, \quad (4.30a)$$

$$\Delta |\dot{\theta}| \ll \frac{1}{4}\Omega_0^2. \quad (4.30b)$$

2. *Global Adiabatic Condition.* This condition comes simply from the integration of equations (4.27) and (4.29). Since the purpose of the STIRAP is to perform total population transfer from $|1\rangle \rightarrow |3\rangle$, the angle θ in $|n_0(t)\rangle$, must go from 0 to $\pi/2$. Hence,

$$\int_0^{t_f} \dot{\theta}(t) dt = \int_0^{\pi/2} d\theta = \frac{\pi}{2}.$$

With that, we obtain that

$$\int_0^{t_f} \Omega(t) dt \gg \frac{\pi}{2}, \quad (4.31a)$$

and

$$\int_0^{t_f} \Omega^2(t) dt \gg 2\Delta\pi. \quad (4.31b)$$

The time integration of a Rabi frequency is called in the literature as the temporal area pulse of the radiation field, $\Theta(t)$ (FOX, 2006).

If we consider these global conditions for the worst case scenario, we obtain an important criteria to choose the total execution time of the protocol. Equations (4.31a) and (4.31b) therefore become

$$\Omega_0 t_f \gg \frac{\pi}{2}, \quad (4.32a)$$

$$\Omega_0^2 t_f \gg 2\pi\Delta, \quad (4.32b)$$

finally obtaining,

$$t_f \gg \frac{\pi}{2\Omega_0}, \quad (4.33a)$$

for the $\Delta \ll \Omega$ regime, and

$$t_f \gg \frac{2\pi\Delta}{\Omega_0^2}, \quad (4.33b)$$

for the $\Delta \gg \Omega$ regime.

4.6 Performing the STIRAP

We now use the results of the previous subsections to determine how the STIRAP protocol is to be performed in practice. The atomic system is initially ($t = 0$) prepared in state $|1\rangle$. This means it is in the eigenstate $|n_0(t)\rangle$, for $\theta = 0$. From the definition of the mixing angles, this requires the pump pulse to be negligibly small at this moment. Then, both pulses are slowly changed over time, obeying the conditions for adiabaticity, until

$\theta = \pi/2$ at $t = t_f$. Since we follow an adiabatic dynamics, the system remained in the eigenstate $|n_0(t)\rangle$, which at the end is equal to state $|3\rangle$, and total population transfer is complete. Again, recurring to the definition of the mixing angles, we see that the Stokes pulse will have to be negligibly small at this final moment. Hence, first the Stokes pulse is sent, then the pump pulse, without total overlap. This is often called ‘counterintuitive ordering’ (KUKLINSKI et al., 1989; VITANOV et al., 2001; SHORE, 2017).

We conveniently choose Gaussian shapes for the pump and Stokes pulses, since they are a preferred shape for experimental implementation (VITANOV et al., 2001). We use the particular form presented in (LI; CHEN, 2016),

$$\Omega_p(t) = \Omega_0 \exp \left[-\frac{(t - t_f/2 - t_0)^2}{\sigma^2} \right], \quad (4.34)$$

$$\Omega_s(t) = \Omega_0 \exp \left[-\frac{(t - t_f/2 + t_0)^2}{\sigma^2} \right], \quad (4.35)$$

where $2t_0$ is the separation time between the maxima of the pulses, Ω_0 the amplitude, and σ the pulse width. These pulses are plotted in fig. 5(a). Here we choose $\Omega_0 = 2\pi \times 3MHz$, $t_f = 10\mu s$, $t_0 = t_f/10$ and $\sigma = t_f/6$. These parameters are set to correspond to existing experimental realisations of the protocol (DU et al., 2016).

Here we choose to work in the resonance condition ($\Delta = 0$), a choice of no particular importance here, but that will become clear in the next chapter. It is important to point out that we sometimes find in the literature the same parameters, but a one-photon detuning of $\Delta = 2\pi \times 2.5Ghz$, and therefore ($\Delta \gg \Omega_0$) (CHEN et al., 2010; LI; CHEN, 2016). This is normally done so that certain simplifications (such as effective Hamiltonians of lower dimensionality) can be used when the associated accelerated protocol is performed. However, for STIRAP itself, this regime is clearly non-adiabatic (from equation (4.33b), $2\pi\Delta/\Omega_0^2 = 100\mu s$, which is not much smaller than $t_f = 400\mu s$), and therefore total population inversion cannot be achieved, as seen in fig. 2 (c) of (LI; CHEN, 2016). A working STIRAP would require increasing the total duration of the protocol or reducing Δ , and we opted for the latter.

Once the value of the one-photon detuning is established, it is easy to check that the value of the other parameters are appropriate. First, eq. (4.33a) establishes a relation between Ω_0 and t_f , which can be seen as somewhat vague (at what point do we consider something as “much greater than” some other thing?). Vitanov (VITANOV et al., 2001) improves this requirement by informing that, when working with coherent pulses, it is sufficient to guarantee that $\Omega_0 t_f \geq 10$. In our choice, their product is 100π , considerably surpassing the criteria. Also, there is no particular requirements for the value of σ , and a

wide range for the choice of t_0 , the restrictions being that the pulses remain counterintuitive, and not completely separated.

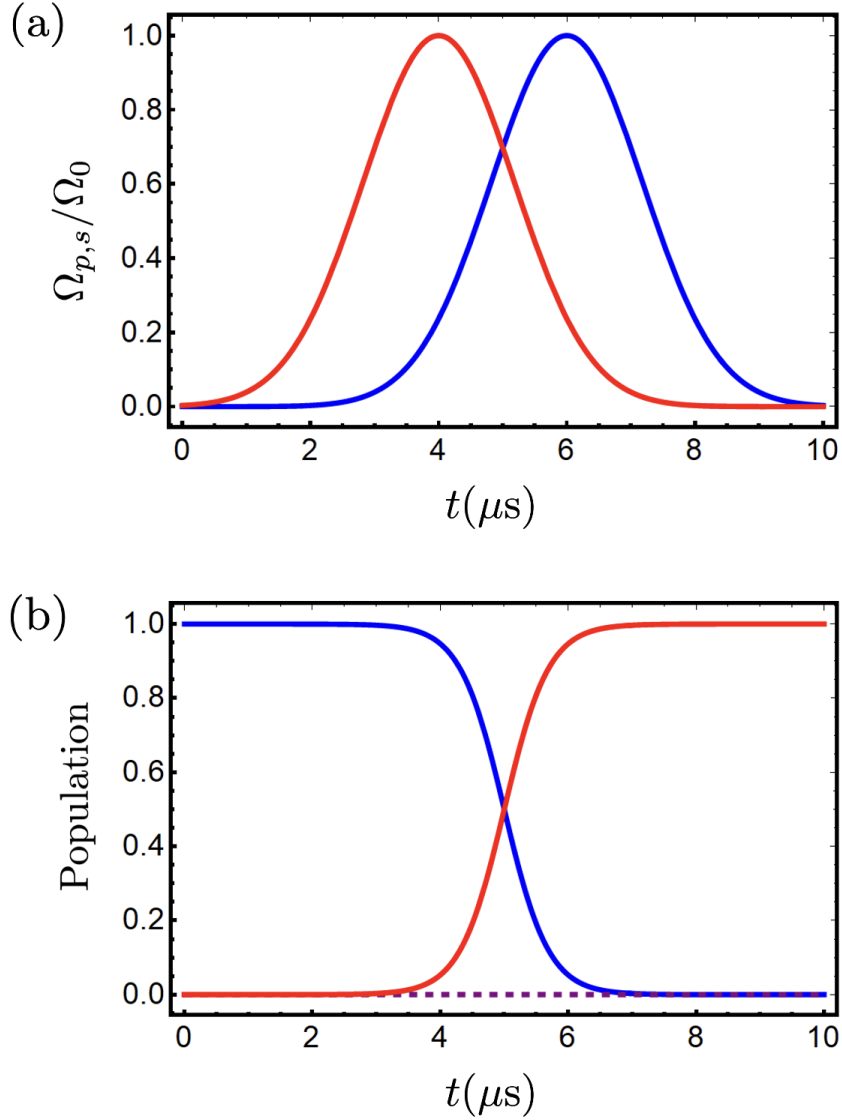


Figure 5 – Time behavior of: (a) the pump (blue) and stokes (red) pulses given by equations (4.34) and (4.35), and (b) the populations of the atomic levels $|1\rangle$ (blue), $|2\rangle$ (purple) and $|3\rangle$ (red), with the initial state given by $|n_0(0)\rangle \approx |1\rangle$. The parameters used are specified in the text.

To confirm that total population transfer is achieved through this process, we analyze the behavior of the probability functions. Since the system remains at the eigenstate $|n_0(t)\rangle$ throughout the process, the value of the populations in time is given by,

$$P_1(t) = |\langle 1|n_0(t)\rangle|^2 = \cos^2 \theta(t), \quad (4.36a)$$

$$P_2(t) = |\langle 2|n_0(t)\rangle|^2 = 0, \quad (4.36b)$$

$$P_3(t) = |\langle 3 | n_0(t) \rangle|^2 = \sin^2 \theta(t), \quad (4.36c)$$

which are plotted in figure 5(b). With this, we conclude the presentation of our reference protocol. One of the tasks of the next chapter is to show how the same results can be obtained faster, through the time-rescaling method.

5 Results

In this chapter we present the results obtained in this work. First, an important proof about the “transitionless” nature of the TR protocol. Then, we propose the actual realization of the speed up of the STIRAP, or *STIRSAP* (Stimulated Raman Shortcut-to-adiabatic passage), through the time-rescaling method. The fidelity and thermodynamic cost are also evaluated.

5.1 Transitionless Proof

In section 3.4, it was shown that the TR method can speed up a reference, adiabatic protocol, taking the system from an eigenstate of the Hamiltonian at $t = 0$ and delivering it back to that eigenstate, at $t = t_f/a$. However, so far, there were no investigations on the nature of the dynamics of the system **during** the application of the TR process, meaning we did not know the route that the system would take in the Hilbert space between initial and final states. This lack of knowledge had particular down side, since, for example, when tracking the populations of the atomic levels in time, one would have to solve a sometimes complicated Schrödinger equation, generally by computational means (ANDRADE; FRANÇA; BERNARDO, 2022). On the other hand, an accelerated protocol with a known route allows for the use of a simpler analytic evaluation, such as in (4.36a), (4.36b) and (4.36c).

In what follows, we propose a simple proof that, actually, the TR protocol drives the system through an evolution route which not only has the same properties of the reference protocol being accelerated (as it was observed in certain applications (BERNARDO, 2020; ANDRADE; FRANÇA; BERNARDO, 2022)), but is indeed the same route. In particular, if the reference is adiabatic, we show that the associated TR protocol is transitionless. This proof can be obtained by means of two independent manners, (i) by a consideration on the nature of the evolution generated by the TR Hamiltonian and (ii) by modifying the proof of the adiabatic theorem, presented in section 3.1.

5.1.1 Analysis of the Evolution created by the TR Hamiltonian

As we have seen in section 3.4, a reference, $\hat{H}(t)$ Hamiltonian generates a unitary time evolution in a closed quantum system, given by eq. (3.22). In the case of the TR Hamiltonian $\hat{\mathcal{H}}(\tau)$, the evolution of the system is given by the evolution operator in eq. (3.23). Since the difference here is a simple change of variables ($t = f(\tau)$), these evolutions produce the same result, and a system initially prepared in state $|\psi_i\rangle$, would arrive at the final state $|\psi_f\rangle$, both by $|\psi_f\rangle = \hat{\mathcal{U}}_{ref}(t_f) |\psi_i\rangle$ and by $|\psi_f\rangle = \hat{\mathcal{U}}_{TR}(f^{-1}(t_f)) |\psi_i\rangle$.

Consider now re-writting eq. (3.22) in terms of a γ parameter, such that

$$\hat{\mathcal{U}}(\gamma t_f) = \hat{\mathcal{T}} \exp \left[-\frac{i}{\hbar} \int_0^{\gamma t_f} \hat{H}(t) dt \right]. \quad (5.1)$$

If we allow γ to vary continuously between 0 and 1, this time evolution operator will transform the initial state $|\psi_i\rangle$ into all possible states $|\psi_\gamma\rangle$ in the path¹ to $|\psi_f\rangle$. For the time rescaled evolution, this re-writting similarly produces

$$\hat{\mathcal{U}}(f^{-1}(\gamma t_f)) = \hat{\mathcal{T}} \exp \left[-\frac{i}{\hbar} \int_0^{f^{-1}(\gamma t_f)} \hat{\mathcal{H}}(\tau) d\tau \right]. \quad (5.2)$$

Again, since the difference between the two evolutions is simply the change of variables $t \rightarrow \tau$, they both produce same state $|\psi_\gamma\rangle$ when applied to the initial state, $|\psi_i\rangle$. It is important to observe that changing of $t_f \rightarrow \gamma t_f$ in eq. (3.25) creates a new rescaling function that fulfills the boundary conditions at $t = 0$ and $t = \gamma t_f$. The conclusion is that the parameter γ characterizes a state which is common both to the reference and the TR processes, which, in turn, means that both evolutions comprise of the same group of intermediate states, or the same path. The difference is merely in the speed in which the system reaches a given state: for the reference, $|\psi_\gamma\rangle$ is reached at $t = \gamma t_f$, and for the TR case, at $t = f^{-1}(\gamma t_f)$. In fig. 6, we plot the changes of a system between $|\psi_i\rangle$ and $|\psi_f\rangle$, supposing a reference process ($a = 1$) and the TR processes with $a = 2$ and $a = 10$, where the rescaling function in eq. (3.25) was used.

We can now explore the transitionless nature of the TR protocol. This property is associated with the adiabatic theorem: a system initially prepared in one of the eigenstates of its Hamiltonian, will remain in this eigenstate throughout an adiabatic process. If this eigenstate is $|n\rangle$, the path followed by the system in this situation is given by the set $\{|n(\gamma t_f)\rangle\}$, $0 \leq \gamma \leq 1$. Now, we consider the commutability between the reference and TR Hamiltonian: since their difference is a change of variables and a scalar function, they must commute:

¹ By “path” we mean the time-trajectory of the state of the system, or the particular sequence of states in the associated Hilbert space that the system follows between the initial and final states.

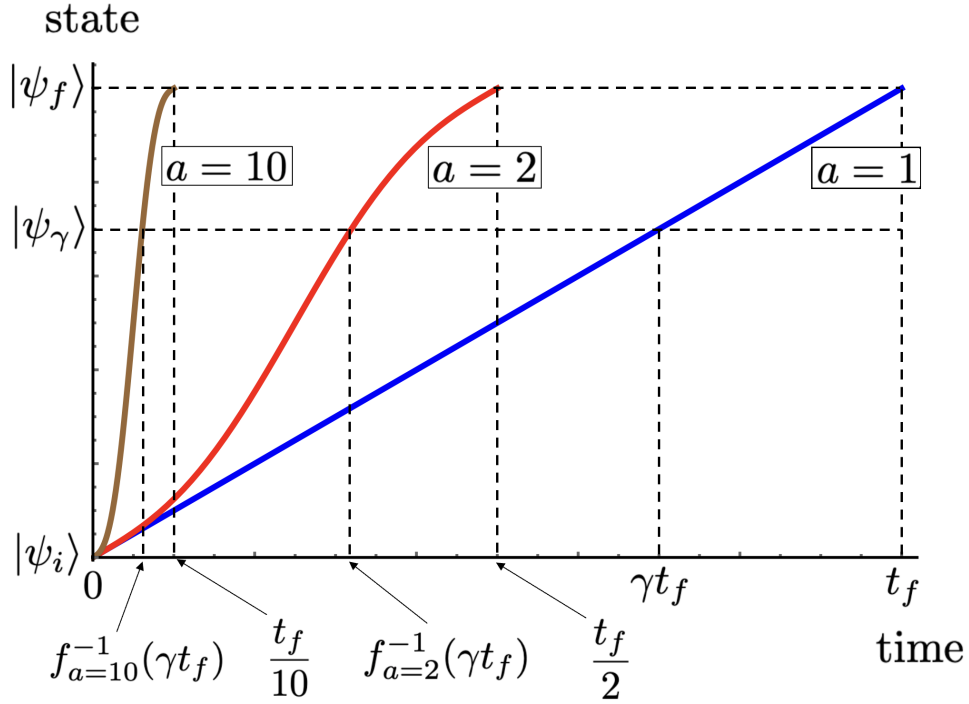


Figure 6 – Time behavior of a general reference process, $a = 1$, and the designed TR processes for $a = 2$ and $a = 10$. The route followed by the quantum system from the initial state $|\psi_i\rangle$ to the final state $|\psi_f\rangle$ through the Hilbert space is the same in all cases. However, the time necessary to reach any state $|\psi_\gamma\rangle$ of the route can be made shorter with increasing a .

$$[\hat{H}(t), \hat{\mathcal{H}}[f^{-1}(t)]] = 0. \quad (5.3)$$

As a consequence, they share a simultaneous set of eigenstates - the set $\{|n(\gamma t_f)\rangle\}$ being also eigenstates of the TR Hamiltonian. Hence, if the reference protocol is transitionless (the system passes only through the same eigenstate of the reference Hamiltonian in different moments of time), the TR protocol evolution, which shares the same path, will promote an evolution where the system remains in a certain eigenstate of the TR Hamiltonian: the time rescaling protocol is also transitionless.

5.1.2 Transitionless Proof via the Adiabatic Theorem

In this second proof, we follow the same path taken in section 3.1 to arrive at the adiabatic theorem, but this time considering a time-rescaled state $|\psi(\tau)\rangle$, evolving under the $\hat{\mathcal{H}}(\tau)$ Hamiltonian.

Consider a closed system in state $|\psi(\tau)\rangle$, which evolves in time through the influence of the time-rescaled Hamiltonian, $\hat{\mathcal{H}}(\tau)$. This evolution must obey the Schrödinger equation, which can be re-written as (3.6),

$$\dot{c}_m(\tau) = -\langle m(\tau)|\dot{m}(\tau)\rangle - \sum_{n \neq m} c_n(\tau) \langle m(\tau)|\dot{n}(\tau)\rangle e^{i(\theta_n - \theta_m)\tau}, \quad (5.4)$$

with $c_n(\tau) = \langle n(\tau)|\psi(\tau)\rangle$. The $|n(\tau)\rangle$ states are eigenstates of a reference Hamiltonian, given by (3.1),

$$\hat{H}(\tau) |n(\tau)\rangle = E_n(\tau) |n(\tau)\rangle, \quad (5.5)$$

where t was changed to τ with no loss of generality. These are also eigenstates of the TR Hamiltonian, since by definition $\hat{\mathcal{H}}(\tau) = \hat{H}(\tau)\dot{f}(\tau)$, yielding

$$\hat{\mathcal{H}}(\tau) |n(\tau) = E_n(\tau)\dot{f}(\tau) |n(\tau)\rangle. \quad (5.6)$$

Now, as it was done in 3.1, the inner products in the second term of (5.4) can be re-written conveniently if we derive equation (5.6),

$$\begin{aligned} \dot{\hat{H}}(\tau)\dot{f}(\tau) |n(\tau)\rangle + \hat{H}(\tau)\ddot{f}(\tau) |n(\tau)\rangle + \hat{H}(\tau)\dot{f}(\tau) |\dot{n}(\tau)\rangle = \\ \dot{E}_n(\tau)\dot{f}(\tau) |n(\tau)\rangle + E_n(\tau)\ddot{f}(\tau) |n(\tau)\rangle + E_n(\tau)\dot{f}(\tau) |\dot{n}(\tau)\rangle, \end{aligned}$$

and apply $\langle m(\tau)|$ ($m \neq n$) on both sides

$$\dot{f}(\tau) \left[\langle m(\tau)|\dot{\hat{H}}(\tau) |n(\tau)\rangle + E_m(\tau) \langle m(\tau)|\dot{n}(\tau)\rangle \right] = \dot{f}(\tau) E_n(\tau) \langle m(\tau)|\dot{n}(\tau)\rangle, \quad (5.7)$$

and since $\dot{f}(\tau)$ multiplies both sides, it will be cancelled. Hence, equation (5.7) becomes equivalent to that obtained if the time evolution was produced through the reference Hamiltonian, and the inner products,

$$\langle m(\tau)|\dot{n}(\tau)\rangle = \frac{\langle m(\tau)|\dot{\hat{H}}(\tau) |n(\tau)\rangle}{E_n(\tau) - E_m(\tau)}. \quad (5.8)$$

Hence, equation (5.4) becomes

$$\dot{c}_m(\tau) = -c_m(\tau) \langle m(\tau)|\dot{m}(\tau)\rangle - \sum_{n \neq m} \frac{\langle m(\tau)|\dot{\hat{H}}(\tau) |n(\tau)\rangle}{E_n(\tau) - E_m(\tau)} c_n(\tau) e^{i(\theta_n - \theta_m)\tau}. \quad (5.9)$$

How can this result be interpreted? If only the first term in (5.9) existed, then $c_n(t)$ would remain the same as $c_n(0)$ (apart from a global phase). Then, all possible transitions are quantified within the second term. That is the same for both the TR and reference protocols. Then, the evolution driven by the TR Hamiltonian conserve the same properties as that of the reference one. In particular, if $\hat{H}(t)$ obeys the adiabatic theorem,

$$\left| \frac{\langle m(\tau) | \dot{\hat{H}}(\tau) | n(\tau) \rangle}{E_n(\tau) - E_m(\tau)} \right| \ll | \langle m(\tau) | \dot{m}(\tau) \rangle |, \quad (5.10)$$

then eq. (5.9) turns into,

$$\dot{c}_m(\tau) \approx -c_m(\tau) \langle m(\tau) | \dot{m}(\tau) \rangle, \quad (5.11)$$

and

$$c_m(\tau) = c_m(0) e^{i\gamma_m(\tau)}. \quad (5.12)$$

If the system starts in one of the eigenstates of $\hat{H}(t)$, it will remain in this eigenstate throughout the application of the TR protocol, which means that, if the TR protocol accelerates an adiabatic one, it will be transitionless.

5.2 Performing the STIRSAP

We are now able to apply the TR method (including the proof of its transitionless feature) to the STIRAP protocol and produce a new type of STIRSAP, or stimulated Raman shortcut-to-adiabatic passage. To do so, we simply follow the steps described in section 3.4. First, we rescale the time variable t in all relevant equations of the STIRAP; they now become functions of the variable τ , with the relation given by equation (3.25):

$$t = a\tau - \frac{t_f}{2\pi a} (a-1) \sin\left(\frac{2\pi a}{t_f} \tau\right). \quad (5.13)$$

Next, the Hamiltonian of the STIRAP in equation (4.14) is modified to become the TR Hamiltonian, following equations (3.24) and (3.26). Since the reference Hamiltonian is composed of three elements, the two pulses $\Omega_p(t), \Omega_s(t)$ and the one-photon detuning Δ , it

is enough to obtain their transformation to create the new Hamiltonian. From equations (4.34), (4.35), we obtain

$$\tilde{\Omega}_p(t) = \Omega_0 \exp \left(\frac{\left[a\tau - \frac{t_f}{2\pi a}(a-1) \sin \left(\frac{2\pi a}{t_f} \tau \right) - t_f/2 - t_0 \right]^2}{\sigma^2} \right) \left[a - (a-1) \cos \left(\frac{2\pi a}{t_f} \tau \right) \right], \quad (5.14a)$$

$$\tilde{\Omega}_s(t) = \Omega_0 \exp \left(\frac{\left[a\tau - \frac{t_f}{2\pi a}(a-1) \sin \left(\frac{2\pi a}{t_f} \tau \right) - t_f/2 + t_0 \right]^2}{\sigma^2} \right) \left[a - (a-1) \cos \left(\frac{2\pi a}{t_f} \tau \right) \right], \quad (5.14b)$$

and

$$\tilde{\Delta}(t) = \frac{\Omega_0}{10} \left[a - (a-1) \cos \left(\frac{2\pi a}{t_f} \tau \right) \right], \quad (5.14c)$$

with the TR Hamiltonian, then, becoming

$$\hat{\mathcal{H}}(\tau) = \frac{\hbar}{2} \begin{pmatrix} 0 & \tilde{\Omega}_p(\tau) & 0 \\ \tilde{\Omega}_p(\tau) & 2\tilde{\Delta}(\tau) & \tilde{\Omega}_s(\tau) \\ 0 & \tilde{\Omega}_s(\tau) & 0 \end{pmatrix}. \quad (5.15)$$

In practical terms, the change requires no additional fields - merely the modulation of the pump and Stokes pulses, as well as adding a time-dependency on the one-photon detuning. This is an important feature to point out, since in the counterdiabatic method, the addition of the $\hat{H}_{CD}(t)$ Hamiltonian into the reference one generally results in the need of extra coupling fields. In reference (LI; CHEN, 2016), for example, a new pulse of Rabi frequency Ω_a is introduced, besides the pump and Stokes. In this particular work, certain special tricks were used to circumvent this necessity and perform the accelerated protocol only in terms of two, modified pulses. However, this may not be the general case, specially when treating more complex systems. In the TR method, however, the requirement of no additional fields is a built-in feature. The manipulation of the amplitude of the pulses is a straightforward laboratory process, obtained by a variety of methods and devices such as the acousto-optic modulator (MEYER et al., 2003).

In order to avoid the extra experimental requirement of (sometimes) fast time-modulation in the one-photon detuning, imposed in eq.(5.14c), we chose to set $\Delta = 0$ in chapter 4, which provides $\tilde{\Delta} = 0$. Moreover, we shall see in the next section that this

resonance condition retains high fidelity in performing population inversion, even when the actual detuning is increased (or decreased) in several MHz.

An important quantity in this new scheme is the contraction parameter a , a measure of how fast we accelerate the STIRAP, and consequently, of how the fields must be modulated. We plot a comparison of the new pulses for the values of $a = 2$ and $a = 10$ in figure 7. Observe that the peak of the rescaled pulses are no longer a constant Ω_0 , but vary linearly with a . Comparing equations (5.14a) and (5.14b) with equations (4.34) and (4.35) at their peak values, we obtain that,

$$\tilde{\Omega}_{peak}^{(p,s)} = \Omega_0(2a - 1). \quad (5.16)$$

Hence, although there is no specific theoretical time limitations given by the TR method itself², there will certainly be practical restrictions associated with the limitations of producing increasingly more intense pulses. For example, given the reference amplitude of $\Omega_0 = 2\pi \times 3$ MHz used in the previous chapter, we have that the new, modulated pulses will arrive peak amplitudes of $\tilde{\Omega}_0 \approx 1$ GHz for $a > 27$, which become increasingly more complicated to be produced in laboratory (HUBER et al., 2011; SHIMADA et al., 2023).

In order to confirm that total population transfer was achieved at the time t_f/a , we must evaluate the time evolution of the populations of the atomic levels. Until now, this would require to solve the Schrödinger equation for the Hamiltonian given in equation (5.15), and then obtain the population functions as explained in section 2.2, through equations (2.8a), (2.8b) and (2.8c), which would have to be done numerically. Now, this is not difficult to do when working with a three-level system. However, as it was explained in the introduction, one of the purposes of this work is to explore the performance of the TR method as we progress to more complicated systems, and we expect increasingly difficulty to solve these equations as we progress to treat larger, N-body problems.

The proof presented in section 5.1, may present some aid in this situation, since we now understand that the application of the TR protocol introduces no transitions. Hence, if the system is initially prepared in the eigenstate $|n_0(0)\rangle = |1\rangle$ of the reference Hamiltonian, it will remain in $|n_0(\tau)\rangle$ at all times. The population of the levels over time may be accessed, then, in a way similar to that of section 4.6, equations (4.36a), (4.36b) and (4.36c), with the difference that the mixing angle $\theta(t)$ needs to be rescaled to become $\tilde{\theta}(\tau)$, defined as $\tan \tilde{\theta}(t) = \tilde{\Omega}_p/\tilde{\Omega}_s$. These new population functions are,

$$\tilde{P}_1(t) = \cos^2[\tilde{\theta}(\tau)], \quad (5.17a)$$

² Besides, of course, a possible limitation imposed by the quantum speed limit (THAKURIA et al., 2024; UHLMANN, 1992), which was not investigated here.

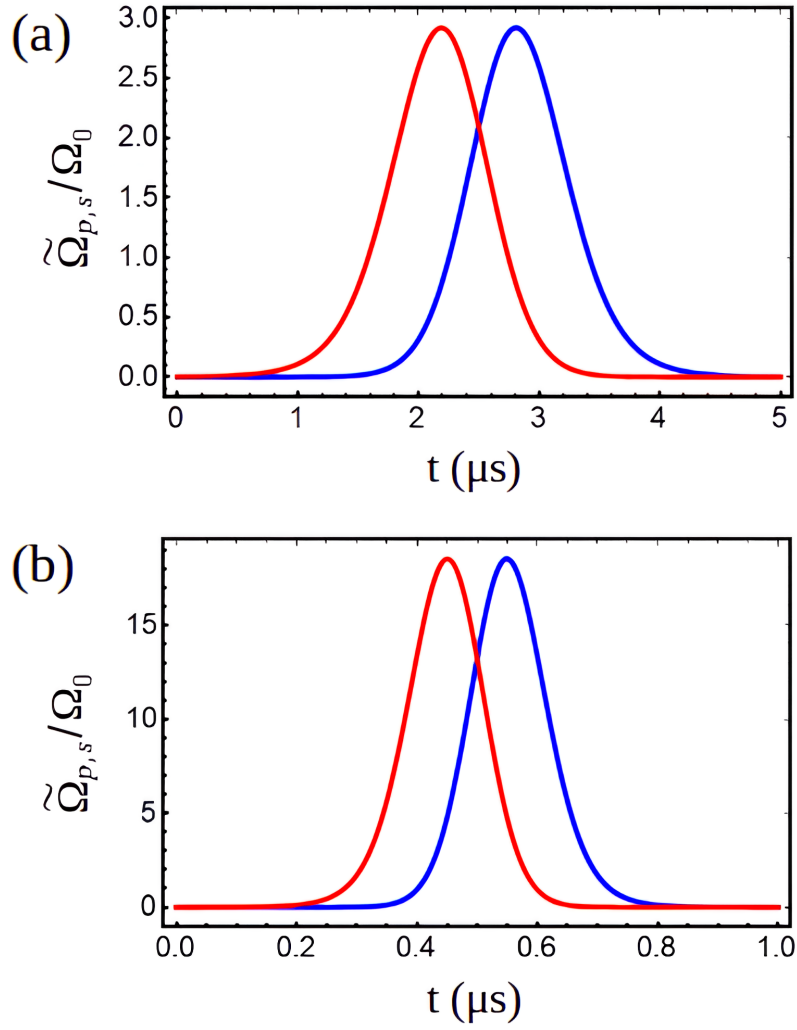


Figure 7 – Behavior of the new pump (blue) and stokes (red) pulses, with the contraction parameter assuming the values of (a) $a = 2$ and (b) $a = 10$. The same parameters of fig. 5 were used. Although the plots closely resemble Gaussian shapes, they are modulated as given in equations (5.14a) and (5.14b).

$$\tilde{P}_2(t) = 0, \quad (5.17b)$$

$$\tilde{P}_3(t) = \sin^2[\tilde{\theta}(\tau)], \quad (5.17c)$$

which are plotted in fig. 8. As desired, total population is achieved without occupying the level $|2\rangle$ at any moment.

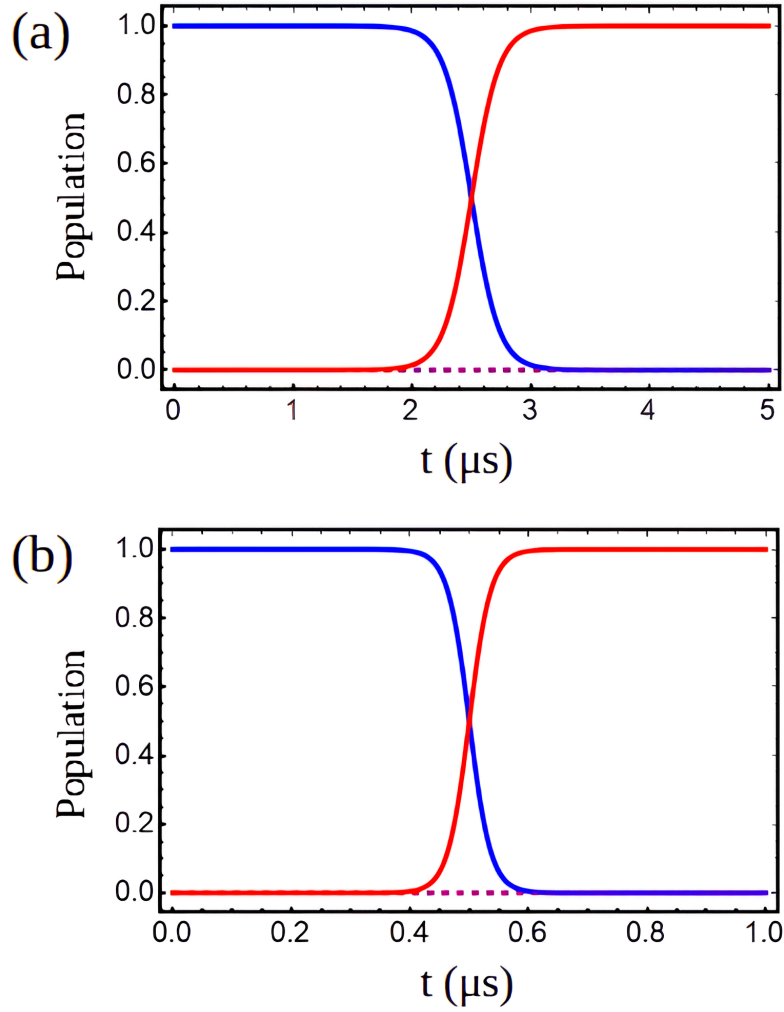


Figure 8 – Time evolution of the populations of levels $|1\rangle$ (blue), $|2\rangle$ (dashed purple) and $|3\rangle$ (red) for the TR passage protocol with the initial state given by $|1\rangle$, and the contraction parameter assuming the values (a) $a = 2$ and (b) $a = 10$. In both cases we observe that the population inversion occurs at least a times faster than in the reference ($a = 1$) protocol, shown in fig. 5. The same parameters of fig. 5 were considered.

5.3 Stability Against Errors

As discussed before, the main objective of any STA is to accelerate a reference, adiabatic protocol, in order to avoid unwanted effects such as decoherence. The reference protocols are expected to be considerably robust against systematic errors, i.e., once the conditions for adiabaticity are met, small changes in experimental parameters do not alter significantly the dynamics of the system through one of the eigenstates of the Hamiltonian. Specially in the case of STIRAP, errors in parameters such as the one-photon detuning, the pulse area and the separation time between pulses, do not significantly alter

the fidelity of the population transfer, as long as the counterintuitive ordering and the conditions of section 4.5 are respected (SHORE, 2017). An example is given in figure 9.

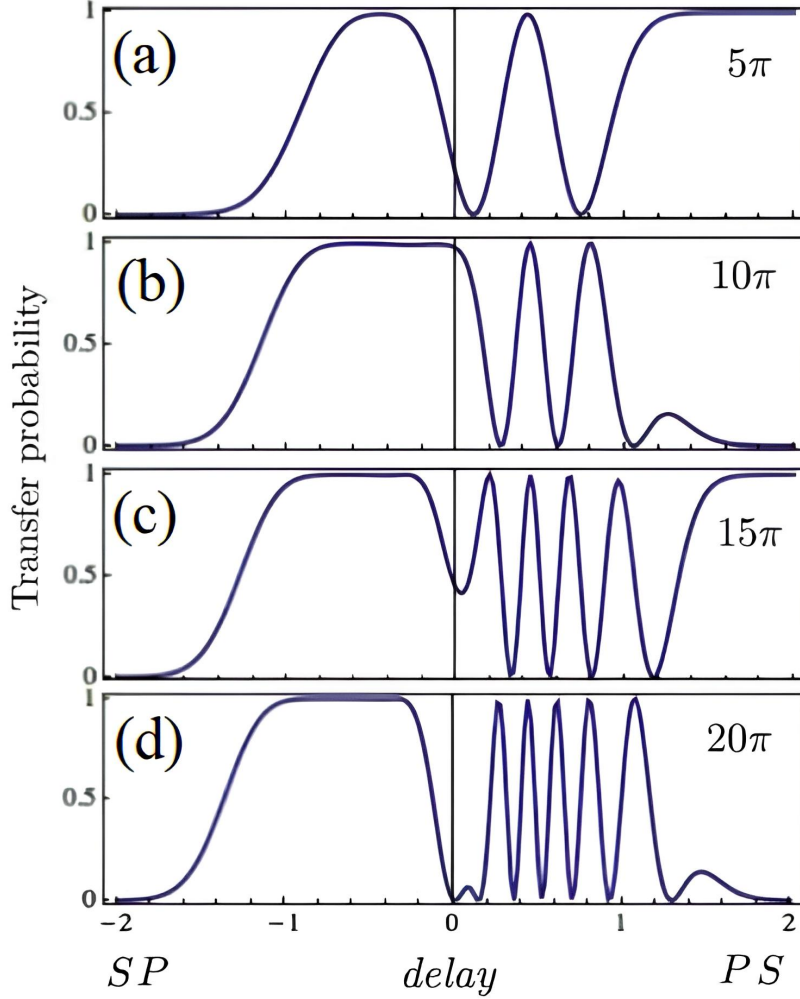


Figure 9 – Probability transfer to state $|3\rangle$ as a function of the delay between pulses, for pulse areas of (a) 5π , (b) 10π , (c) 15π and (d) 20π . Gaussian pulses in the form described in eqs. (4.34) and (4.35) were used, with $\Delta = 0$. Observe that in all cases, there is a wide plateau within which the protocol is performed with high fidelity, regardless of changes in the delay. Image taken from (SHORE, 2017).

Hence, in attempting to perform an accelerated protocol, care must be taken so that an increase in speed does not come at the cost of loss of robustness. In other words, no considerable decrease in fidelity should occur due to small changes in the parameters involved - a consequence of the unavoidable errors in experimental manipulation. This section is dedicated to analyze the fidelity of the TR-based STIRSAP with the change of certain parameters. We shall compare its results to those of the counterdiabatic method, in order to see which approach provides a more robust protocol.

First of all, it is important to explain that, in the literature, fidelity is defined as a measure of “similarity” between the desired and the achieved states, being given by

(BENENTI et al., 2019),

$$F = \langle \psi_{de} | \hat{\rho}_{ob} | \psi_{de} \rangle, \quad (5.18)$$

where $|\psi_{de}\rangle$ denotes the desired state and $\hat{\rho}_{ob}$ is the density matrix of the state obtained at the end of the process. In the present case, the desired state is evidently $|3\rangle$. The STIRSAP process produced by the time rescaling method delivers the final state $|n_0(t_f/a)\rangle$, with associated density matrix $\hat{\rho}_{ob} = |n_0(t_f/a)\rangle \langle n_0(t_f/a)|$. Therefore, eq. (5.18) becomes,

$$F = \langle 3 | n_0(t_f/a) \rangle \langle n_0(t_f/a) | 3 \rangle = |\langle 3 | n_0(t_f/a) \rangle|^2, \quad (5.19)$$

and from eq. (5.17c),

$$F = \tilde{P}_3(t_f/a). \quad (5.20)$$

A last remark must be made on how the comparisons with the counterdiabatic method will be done. We shall consider the general Hamiltonian of the STIRAP protocol given by eq. (4.14), but with modified pump and Stokes pulses as provided by the CD method, analogously to what we did with the TR method. For the resonance condition, our regime of choice, we can use the modified pulses provided by equations (21) and (22) of reference (LI; CHEN, 2016),

$$\Omega_p^{(cd)} = \sqrt{\Omega_p^2 + 4\Omega_a^2}, \quad (5.21a)$$

$$\Omega_s^{(cd)} = \Omega_s - 2\dot{\phi}^{(cd)}(t), \quad (5.21b)$$

with $\Omega_{p,s}$ given by eqs. (4.34) and (4.35), $\Omega_a = \dot{\theta}(t)$, with $\dot{\theta}$ given by eq. (4.25), and $\phi^{(cd)} = \arctan[2\Omega_a/\Omega_p]$. We then numerically solve the Schrödinger equation for this Hamiltonian, using the *ParametricNDSolve* built-in function from Mathematica to specifically obtain the probability amplitudes for the three energy levels at the final desire time. Then, we just take the square modulus of the amplitude of level $|3\rangle$, and obtain $F = P_3(t'_f)$. We set $t'_f = t_f/a$ to compare these results with those obtained from the TR method through eq. (5.20). Once these general definitions are presented, we can now proceed to the evaluations.

The first parameter against which fidelity is analyzed is the separation time (or delay) between the pump and Stokes pulses. Knowing that $t_{sep} = 2t_0$, we simply assume

the change $t_0 \rightarrow t_0(1 + \epsilon)$, with ϵ being the error parameter. The behavior of F against ϵ is plotted in figure 10. We observe that the time-rescaling STIRASP holds maximum fidelity for the whole range, outperforming the counterdiabatic method in the region of smaller delay.

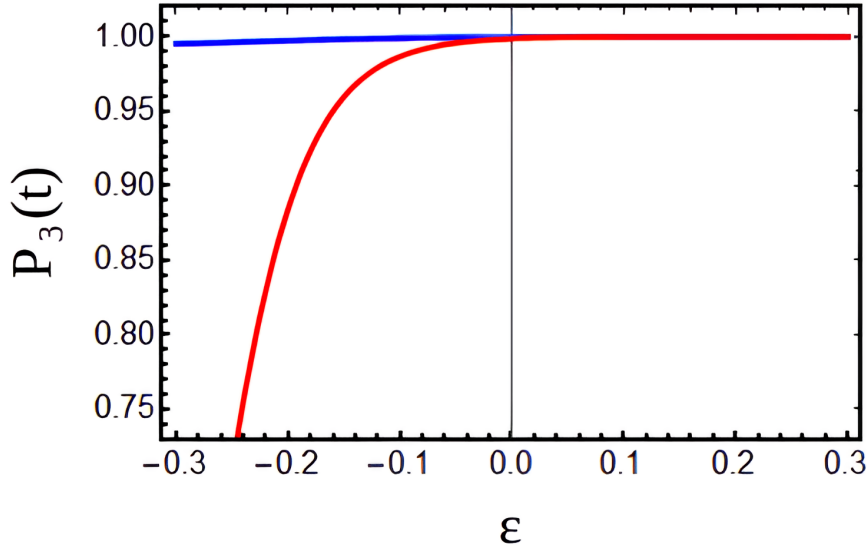


Figure 10 – Behavior of the fidelity of the TR STIRASP (blue) and counterdiabatic STIRASP (red) against errors in the separation time between pulses. We used the same parameters of fig. 5, with the exception of the original t_0 of the counterdiabatic protocol, taken as $t_0 = t_f/8$ for optimization.

We now analyze how fidelity is affected by errors in the amplitude of the pulses. This is simply done by allowing the change $\Omega_{p,s} \rightarrow \Omega_{p,s}(1 + \beta)$, with β being the error parameter. The behavior of F against β is plotted in figure 11(a). In addition to the TR and counterdiabatic accelerated inversions, we also plot the fidelity of a direct population inversion between $|1\rangle \rightarrow |3\rangle$, performed by a π pulse. Again, the TR STIRASP maintains total fidelity throughout the range of error, outperforming the counterdiabatic method for both increasing or decreasing values of amplitude, as well as the π pulse. In both the amplitude and delay evaluations, the resonance condition was considered for all methods.

We finally analyze how fidelity changes when we relax the resonance condition ($\Delta = 0$), for the TR method, counterdiabatic method and the application of π pulse. This time, we consider not a error parameter, but a variation in the absolute value of the one-photon detuning of $\delta\Delta$. Figure 11(b) shows F against $\delta\Delta$, where we again see the superiority of the TR STIRASP in comparison with the other methods.

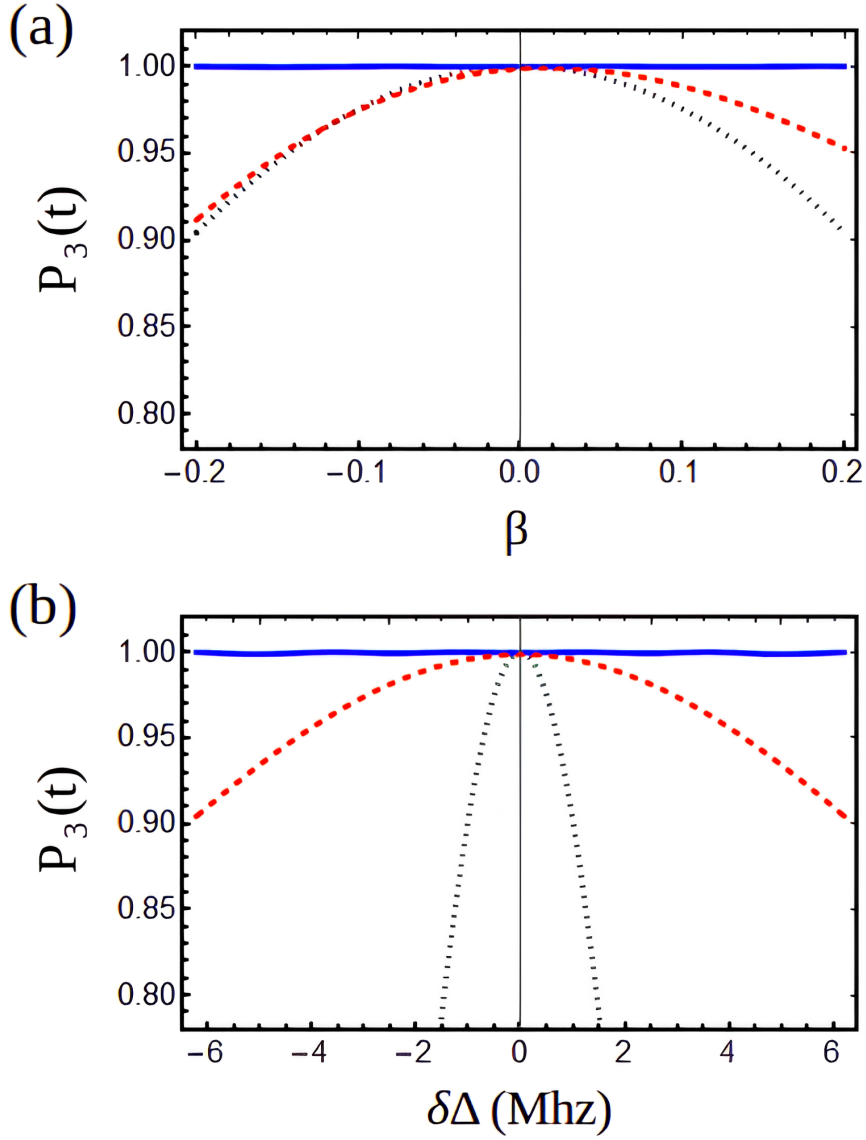


Figure 11 – Behavior of the fidelity of the TR STIRSAP (blue), counterdiabatic STIRSAP (red) and direct two-level population inversion via π pulse (black) for (a) variations in the amplitude of the pulses and (b) variations in the one-photon detuning. The same parameters of fig. 10 were used.

5.4 Thermodynamic Cost

5.4.1 Two-point Measurement Method

Besides speed and fidelity, a third important feature of a good STA is to have the least additional thermodynamic cost to be performed, when compared to the reference protocol. Differences in cost can be an important factor when considering which STA to use in a particular experiment.

Here we shall calculate the average and standard deviation of the work cost of

performing any given protocol through the framework of a “two-point measurement” (TPM) (CAMPISI; HÄNGGI; TALKNER, 2011), following the steps given in (RIBEIRO; LANDI; SEMIÃO, 2016). Since we are working with a closed system, this turns out to be the total thermodynamic cost.

Consider a system which is initially ($t = 0$) in thermal equilibrium with a heat bath at temperature T , such that its initial state is a Gibbs thermal state given by,

$$\hat{\rho}(0) = \sum_n \frac{e^{-\beta E_n^i}}{Z} |n\rangle \langle n|, \quad (5.22)$$

with $Z = \sum_n e^{-\beta E_n^i}$ being the partition function, $\beta = 1/k_b T$ (k_b is the Boltzmann constant) and E_n^i and $|n\rangle$ being the eigenvalues and eigenstates of the initial Hamiltonian, that satisfies

$$\hat{H}_i |n\rangle = E_n^i |n\rangle. \quad (5.23)$$

The first step consists in performing an energy measurement in this initial state, which will yield one of the eigenvalues E_n^i with probability $P_n^i = \langle n | \hat{\rho}(0) | n \rangle = e^{-\beta E_n^i} / Z$. After the measurement, the state of the system collapses in the associated eigenstate, $|n\rangle$.

Next, we isolate the system from the heat bath and apply the desired protocol, so that the system evolves according to a evolution operator $\hat{U}(t_f)$. At the end of the process ($t = t_f$), we perform a second energy measurement, the result being one the eigenvalues E_m^f of the final Hamiltonian, \hat{H}_f , satisfying,

$$\hat{H}_f |m\rangle = E_m^f |m\rangle, \quad (5.24)$$

with probability $P_m^f = |\langle m | \hat{U}(t_f) | n \rangle|^2$. Again, after the measurement the state of the system collapses in the associated eigenstate, $|m\rangle$. Since the whole protocol was applied while the system was isolated from its environment, the first law of thermodynamics tells us that,

$$W = \Delta U,$$

$$W = E_m^f - E_n^i. \quad (5.25)$$

It is important to notice that, given the existence of intrinsic quantum fluctuations (and possible thermal fluctuations), work must also be a fluctuating quantity. In other words, equally performed experiments will result in different possible values of work. Since

work becomes a random variable, we can derive some statistically useful information, such as its average and standard deviation.. To do so, we first associate to the spectrum of possible results of eq. (5.25), a probability distribution function given by,

$$P(W) = \sum_{n,m} P_m^f P_n^i \delta[W - (E_m^f - E_n^i)], \quad (5.26)$$

with $\delta(x)$ being the Dirac delta function. We then take the Fourier transform of eq. (5.26), which is easier to work with:

$$\chi(r) = \int_{-\infty}^{+\infty} P(W) e^{irW} dW = \langle e^{irW} \rangle. \quad (5.27)$$

The application of eq. (5.26) in (5.27) provides,

$$\begin{aligned} \chi(r) &= \sum_{n,m} \int_{-\infty}^{+\infty} P_m^f P_n^i \delta[W - (E_m^f - E_n^i)] e^{irW} dW, \\ \chi(r) &= \sum_{n,m} P_m^f P_n^i e^{ir(E_m^f - E_n^i)}, \\ \chi(r) &= \sum_{n,m} |\langle m | \hat{U}(t_f) | n \rangle|^2 \left(\frac{e^{-\beta E_n^i}}{Z} \right) e^{irE_m^f} e^{-irE_n^i}, \\ \chi(r) &= \sum_{n,m} \langle n | \hat{U}^\dagger(t_f) e^{irE_m^f} | m \rangle \langle m | \hat{U}(t_f) e^{-irE_n^i} \left(\frac{e^{-\beta E_n^i}}{Z} \right) | n \rangle. \end{aligned} \quad (5.28)$$

By considering equations (5.22), (5.23), and (5.24), eq. (5.28) becomes

$$\begin{aligned} \chi(r) &= \sum_{n,m} \langle n | \hat{U}^\dagger(t_f) e^{ir\hat{H}_f} | m \rangle \langle m | \hat{U}(t_f) e^{-ir\hat{H}_i} \hat{\rho}(0) | n \rangle \\ \chi(r) &= \sum_n \langle n | \hat{U}^\dagger(t_f) e^{ir\hat{H}_f} \hat{U}(t_f) e^{-ir\hat{H}_i} \hat{\rho}(0) | n \rangle, \\ \chi(r) &= Tr\{\hat{U}^\dagger(t_f) e^{ir\hat{H}_f} \hat{U}(t_f) e^{-ir\hat{H}_i} \hat{\rho}(0)\}. \end{aligned} \quad (5.29)$$

To proceed, we observe that the last term in eq. (5.27) allows us to re-write $\chi(r)$ in terms of the statistical moments of W , obtaining,

$$\chi(r) = 1 + ir \langle W \rangle - \frac{r^2}{2} \langle W^2 \rangle + \mathcal{O}(r^3). \quad (5.30)$$

We can also expand the exponential terms in eq. (5.29),

$$e^{ir\hat{H}_f} = 1 + ir\hat{H}_f - \frac{r^2}{2}\hat{H}_f^2 + \mathcal{O}(r^3), \quad (5.31a)$$

$$e^{-ir\hat{H}_i} = 1 - ir\hat{H}_i - \frac{r^2}{2}\hat{H}_i^2 + \mathcal{O}(r^3), \quad (5.31b)$$

and insert them into eq. (5.29) to obtain,

$$\chi(r) = Tr\{\hat{U}^\dagger \left(1 + ir\hat{H}_f - \frac{r^2}{2}\hat{H}_f^2 + \dots\right) \hat{U} \left(1 - ir\hat{H}_i - \frac{r^2}{2}\hat{H}_i^2 + \dots\right) \hat{\rho}(0)\},$$

$$\begin{aligned} \chi(r) = Tr\{\hat{U}^\dagger \hat{U} \hat{\rho}(0)\} &+ Tr\{\hat{U}^\dagger (ir\hat{H}_f) \hat{U} \hat{\rho}(0)\} + Tr\{\hat{U}^\dagger \hat{U} (-ir\hat{H}_i) \hat{\rho}(0)\} + Tr\{\hat{U}^\dagger (ir\hat{H}_f) \hat{U} \\ &(-ir\hat{H}_i) \hat{\rho}(0)\} + Tr\{\hat{U}^\dagger \left(-\frac{r^2}{2}\hat{H}_f^2\right) \hat{U} \hat{\rho}(0)\} + Tr\{\hat{U}^\dagger \hat{U} \left(-\frac{r^2}{2}\hat{H}_i^2\right) \hat{\rho}(0)\} + \dots \end{aligned}$$

Since the operation of trace remains invariant under cyclical permutations, we can rearrange the terms in the second and fifth terms to obtain,

$$\begin{aligned} \chi(r) = Tr\{\hat{U}^\dagger \hat{U} \hat{\rho}(0)\} &+ ir[Tr\{\hat{H}_f \hat{U} \hat{\rho}(0) \hat{U}^\dagger\} - Tr\{\hat{U}^\dagger \hat{U} \hat{H}_i \hat{\rho}(0)\}] - \frac{r^2}{2}[Tr\{\hat{H}_f^2 \hat{U} \hat{\rho}(0) \hat{U}^\dagger\} + \\ &+ Tr\{\hat{U}^\dagger \hat{U} \hat{H}_i^2 \hat{\rho}(0)\} - 2Tr\{\hat{U}^\dagger \hat{H}_f \hat{U} \hat{H}_i \hat{\rho}(0)\}] + \mathcal{O}(r^3). \end{aligned}$$

Considering that $\hat{\rho}(t) = \hat{U} \hat{\rho}(0) \hat{U}^\dagger$ and $\langle \hat{A} \rangle = Tr\{\hat{A} \hat{\rho}\}$ (SAKURAI; NAPOLITANO, 2021), we have that

$$\chi(r) = 1 + ir[\langle \hat{H}_f \rangle_{t_f} - \langle \hat{H}_i \rangle_{t_0}] - \frac{r^2}{2}[\langle \hat{H}_f^2 \rangle_{t_f} + \langle \hat{H}_i^2 \rangle_{t_0} - 2Tr\{\hat{U}^\dagger \hat{H}_f \hat{U} \hat{H}_i \hat{\rho}(0)\}] + \mathcal{O}(r^3), \quad (5.32)$$

where $\langle \rangle_{t_i}$ means the average taken at $t = t_i$, with $\hat{\rho} = \hat{\rho}(t_i)$.

By comparing equations (5.29) and (5.32), we obtain,

$$\langle W \rangle = \langle \hat{H}_f \rangle_{t_f} - \langle \hat{H}_i \rangle_{t_0}, \quad (5.33)$$

which is the average work cost, and

$$\langle W^2 \rangle = \langle \hat{H}_f^2 \rangle_{t_f} + \langle \hat{H}_i^2 \rangle_{t_0} - 2Tr\{\hat{U}^\dagger \hat{H}_f \hat{U} \hat{H}_i \hat{\rho}(0)\}. \quad (5.34)$$

Now, since the standard deviation is defined by

$$\Delta W = \sqrt{\langle W^2 \rangle - \langle W \rangle^2}, \quad (5.35)$$

we obtain from equations (5.33) and (5.34) that,

$$\begin{aligned} \Delta W &= \sqrt{\langle \hat{H}_f^2 \rangle_{t_f} + \langle \hat{H}_i^2 \rangle_{t_0} - 2Tr\{\hat{U}^\dagger \hat{H}_f \hat{U} \hat{H}_i \hat{\rho}(0)\} - \langle \hat{H}_f \rangle_{t_f}^2 - \langle \hat{H}_i \rangle_{t_0}^2 + 2\langle \hat{H}_f \rangle_{t_f} \langle \hat{H}_i \rangle_{t_0}}, \\ \Delta W &= \sqrt{\langle (\Delta \hat{H}_f)^2 \rangle_{t_f} + \langle (\Delta \hat{H}_i)^2 \rangle_{t_0} + 2[\langle \hat{H}_f \rangle_{t_f} \langle \hat{H}_i \rangle_{t_0} - Tr\{\hat{U}^\dagger \hat{H}_f \hat{U} \hat{H}_i \hat{\rho}(0)\}]}. \end{aligned} \quad (5.36)$$

5.4.2 Evaluation of Cost for Reference and TR Protocols

In section 3.4 we showed that one of the necessary features to construct the TR Hamiltonian is that it coincides with the reference Hamiltonian at the beginning and at the end of the protocol. Also, in section (5.1), we showed that the time evolutions associated with the reference and TR protocols are equivalent. Analyzing eqs. (5.33) and (5.36) under this light allows us to conclude, then, that

$$\langle W \rangle_{TR} = \langle W \rangle_{ref}, \quad (5.37)$$

and

$$\Delta W_{TR} = \Delta W_{ref}. \quad (5.38)$$

Hence, there is no extra thermodynamic cost in performing a TR accelerated protocol, when compared to the reference one. These are general results, applicable to any protocol designed via the time-rescaling method. They were first demonstrated in (ANDRADE; FRANÇA; BERNARDO, 2022).

It is important to connect these results with our object of study - the acceleration of the STIRAP. First, although the Hamiltonian of the STIRAP comprizes atom + external radiation, the measurements are only performed in the system, so that eqs. (5.33) and (5.36) must be evaluated according to the undisturbed Hamiltonian of the atom. From eq. (4.7), and considering the two-photon resonance condition,

$$\hat{H}_{atom} = \begin{pmatrix} E_1 & 0 & 0 \\ 0 & E_2 & 0 \\ 0 & 0 & E_3 \end{pmatrix}. \quad (5.39)$$

Next, we cannot work with an initial thermal state. Hence, upon realizing the first energy measurement in an ensemble of equally prepared systems, we can only use those whose measurement results are 0 - meaning that the post-measurement state (and our initial state to apply the protocol) is $|1\rangle \equiv |n_0(0)\rangle$ ³ (see section 4.4). Also, at the end of the protocol, the state obtained is pure and an eigenstate of the final Hamiltonian, meaning that there is only one possible value for the second energy measurement: E_3 (since $|n_0(t_f)\rangle \equiv |3\rangle$). The lack of quantum uncertainty results in,

$$\Delta W_{TR/ref} = 0. \quad (5.40)$$

From this and from equation (5.33), we conclude simply that,

$$\langle W \rangle_{TR/ref} \equiv W = E_3 - E_1, \quad (5.41)$$

or, in terms of the frequencies of the external pump and Stokes radiation fields exerting work in the system,

$$W = \hbar(\omega_p - \omega_s). \quad (5.42)$$

³ Since level $|1\rangle$ has the lowest energy, working at low temperatures increases the probability of obtaining it upon first measurement (see equation (5.22)).

6 Conclusion

The adiabatic theorem is a useful tool of control in quantum dynamics. Once it is satisfied, it guarantees that a system starting in a given eigenstate of its Hamiltonian, will be kept in this same eigenstate throughout the process, a feature desirable in several protocols. However, the large times required to follow the adiabatic protocol, result in undesirable effects such as decoherence. In this lies the usefulness of Shortcuts to adiabaticity, methods which allow the preservation of useful adiabatic properties, but acting during much shorter time periods.

In this work we analyzed in more detail the time-rescaling (TR) protocol. It is a considerably simple method to perform a STA, since it requires no knowledge of the instantaneous eigenstates of the reference Hamiltonian, but merely its modification through a suitable rescaling function. An apparent complication of this method was that, if the system started in an eigenstate of the reference Hamiltonian, it guaranteed that it would return to that same eigenstate at the end of the process, but not that it would remain in the eigenstate throughout the process. This could give rise to possible transitions along the process, which would require solving the sometimes complicated Schrödinger equation when attempting to obtain the behavior of the system during the protocol.

Our first important result was to show that such complication is not real. Through the transitionless proof in section 5.1, it was shown that the system follows, through a TR-driven dynamics, the same path as the reference protocol and more, that if this reference obeyed the adiabatic theorem, there were no transitions between eigenstates during the application of the TR-based protocol. This allows us not only to know the route of the system in Hilbert space, but also the time behavior of the population of the states during the protocol in simpler ways, such as known probability functions obtained in the reference case. This seems to be the last piece to show that the TR method has no down-sides when compared to the counterdiabatic method, and is a viable and competitive approach to generate different types of accelerated dynamics.

The second important result was to successfully apply the machinery of the TR dynamics to speed up the STIRAP protocol, the most efficient method to adiabatically perform total population inversion in three-level systems. We showed that such realization requires a simple modulation of the laser pulses of the reference protocol, and a modulation of the one-photon detuning (becoming even experimentally simpler by choosing to work in the resonance condition, $\Delta = 0$). Since the amplitudes of the new pulses increase with the contraction parameter a , there is a practical restriction on how fast the protocol can be performed, tied with the intensity achievable in lasers. However, this restriction becomes

important only for values of a up to 30, when the protocols reach an operation time of a few nanoseconds.

We also analyzed two important characteristics of this new speed up protocol: the fidelity and thermodynamic cost. For the fidelity, it was shown to remain high upon systematic errors in experimental parameters such as the delay between pulses, the pulses' amplitudes and variations of detuning, provided that the counterintuitive ordering and adiabatic conditions (for the reference protocol) were preserved. By comparing it with the counterdiabatic case and the direct inversion via π pulse, the TR protocol was shown to be the most robust among them. The brief discussion of thermodynamic cost made use of the two-point measurement technique, and showed that both the TR and the counterdiabatic STIRSAPs have the same average work than the reference protocol, being equivalent when choosing which protocol to use based on energetic cost.

These results warrant concluding that fast, total population inversion can be achieved with high fidelity, no additional fields and no additional thermodynamic cost through a TR dynamics. The method, then, becomes one of the available tools in the literature to generate controlled population changes in atomic systems, a fundamental feature in preparing qubit states or constructing logical gates in quantum computers. Further, we added to the simplicity of the TR method, the additional feature of being transitionless.

Apart from the merits in its own results, it is expected that this work can motivate further investigations into the properties of the TR method, as well as its application in more complex problems, where no (or harder) solutions to promote accelerated controlled dynamics exist. The article resulting from this work was submitted for publication under the title "Shortcuts to adiabaticity designed via time-rescaling follow the same transitionless route", and is currently available in Preprint ([FERREIRA et al., 2024](#)).

Bibliography

AGNESI, A.; REALI, G. *Encyclopedia of Condensed Matter Physics*. 2. ed. [S.l.]: Elsevier, 2024. v. 4. Citado na página [15](#).

ANDRADE, J. S.; FRANÇA, A. F. S.; BERNARDO, B. L. Shortcuts to adiabatic population inversion: stability and thermodynamic cost. *Sci. Re p.*, v. 12, n. 11538, 2022. Citado 4 vezes nas páginas [15](#), [32](#), [51](#), and [68](#).

ASSÉMAT, E. Hamiltonian singularities in the stirap process. *Presentation at Weizmann Institute of Science*, n. 3-5, 2013. Citado na página [37](#).

AVRON, J. E.; SEILLER, R.; YAFFE, L. G. Adiabatic theorems and applications to the quantum hall effect. *Comm. Math. Phys.*, v. 110, n. 33-49, 1987. Citado na página [26](#).

BENENTI, G. et al. *Principles of Quantum Computation and Information: A Comprehensive Textbook*. 2. ed. [S.l.]: World Scientific Publishing Company, 2019. v. 1. Citado 2 vezes nas páginas [15](#) and [61](#).

BERGMANN, K. et al. Roadmap on stirap applications. *J. Phys. B: Ato. Mol. Phys.*, v. 52, n. 202001, 2017. Citado na página [35](#).

BERGMANN, K.; VITANOV, N. V.; SHORE, B. W. Perspective: stimulated raman adiabatic passage, the status after 25 years. *J. Chem. Phys.*, v. 142, n. 170901, 2015. Citado na página [40](#).

BERNARDO, B. L. Time-rescaled quantum dynamics as a shortcut to adiabaticity. *Phys. Rev. Res.*, v. 2, n. 013133, 2020. Citado 4 vezes nas páginas [14](#), [27](#), [32](#), and [51](#).

BERRY, M. V. Transitionless quantum driving. *J. Phys. A: Math. Theo.*, v. 42, n. 36, 2009. Citado na página [27](#).

BORN, M.; FOCK, V. Proof of the adiabatic theorem. *Zei. für Phy.*, v. 51, n. 165-180, 1928. Citado na página [23](#).

BOSSMANN, L.; GRUMMT, R.; MARTIN, K. On the dipole approximation with error estimates. *Lett. Math. Phys.*, v. 108, p. 185–193, 2018. Citado na página [19](#).

BRASLAVISKY, E. *Glossary of Terms Used in Photochemistry*. 1. ed. [S.l.]: IUPAC, 2007. Citado na página [20](#).

CAMPISI, M.; HÄNGGI, P.; TALKNER, P. P. colloquium: Quantum fluctuation relations: Foundations and applications. *Rev. Mod. Phys.*, v. 83, n. 771-791, 2011. Citado na página [64](#).

CHEN, B.; WANG, J.; ZHOU, Y. Quantum control and its application: A brief introduction. *J. Phys.: Conf. Ser.*, v. 1802, n. 022068, 2021. Citado na página [13](#).

CHEN, X. et al. Shortcut to adiabatic passagem in two and three-level atoms. *Phys. Rev. Lett.*, v. 105, n. 12003, 2010. Citado 2 vezes nas páginas [29](#) and [47](#).

CHEN, X.; MUGA, J. G. Engineering of fast population transfer in three-level systems. *Phys. Rev. A*, v. 86, n. 033405, 2012. Citado na página 29.

CHEN, X. et al. Fast optimal frictionless atom cooling in harmonic traps: Shortcuts to adiabaticity. *Phys. Rev. Lett.*, v. 104, n. 6, 2010. Citado na página 26.

CHEN, Y. et al. Shortcuts to adiabaticity for the quantum rabi model: efficient generation of giant entangled cat states via parametric amplification. *Phys. Rev. Lett.*, v. 126, n. 2, 2021. Citado na página 29.

COURTEILLE, P. W. Atom-light interaction and basic applications. *Lecture Notes, ICTP-SAIFR School on Interaction of Light with Cold Atoms*, p. 7–10, 2023. Citado na página 17.

COUVERT, A. et al. Optimal transport of ultracold atoms in the non-adiabatic regime. *Europhys. Lett.*, v. 83, n. 13001, 2008. Citado na página 13.

DAVIS, W. A.; METCALF, H. J.; PHILLIPS, W. D. Vanishing electric dipole transition moment. *Phys. Rev. A*, v. 19, n. 700, 1979. Citado na página 43.

DEMIRPLAK, M.; RICE, S. A. Adiabatic population transfer with control fields. *J. Phys. Chem. A*, v. 107, n. 46, 2009. Citado 2 vezes nas páginas 26 and 27.

DIAL, O. Eagle's quantum performance progress. 2022. Disponível em: <<https://www.ibm.com/quantum/blog/eagle-quantum-processor-performance,22April2024>>. Citado na página 13.

DJOTYAN, G. P. et al. Population transfer in three-level λ atoms with doppler-broadened transition lines by a single frequency-chirped short laser pulse. *Jour. J. Opt. Soc. Am. B.*, v. 17, n. 107-113, 2000. Citado na página 35.

DOERY, M. R. et al. Population accumulation in dark states and subrecoil laser cooling. *Phys. Rev. A*, v. 52, n. 2295, 1995. Citado na página 43.

DU, Y. et al. Experimental realization of stimulated raman shortcut-to-adiabatic passage with cold atoms. *Nat. Commun.*, v. 7, n. 12479, 2016. Citado na página 47.

FARHI, E. et al. Quantum computation by adiabatic evolution. arXiv:quant-ph/0001106, 2000. Citado na página 13.

FERREIRA, J. L. M. et al. Shortcuts to adiabaticity designed via time-rescaling follow the same transitionless route. *arXiv:2406.07433 [quant-ph]*, 2024. Citado na página 70.

FOX, M. *Quantum Optics, An Introduction*. 1. ed. [S.l.]: Oxford University Press, 2006. Citado 2 vezes nas páginas 21 and 46.

FRANÇA, A. F. S.; ANDRADE, J. S.; BERNARDO, B. L. Speeding up quantum dynamics by adding tunable time-dependent hamiltonians. *Quant. Inf. Proc.*, v. 21, n. 171, 2022. Citado na página 27.

FUJII, K. Introduction to the rotating wave approximation: two coherent oscillations. *Jour. Mod. Phys.*, v. 48, n. 12, 2017. Citado na página 38.

FÜRST, H. A. et al. Controlling the transport of an ion: classical and quantum mechanical solutions. *N. Jou. Phys.*, v. 16, n. 075007, 2014. Citado na página 13.

- GARDINER, D. J.; GRAVES, P. R. *Practical Raman Spectroscopy*. 1. ed. [S.l.]: Springer-Verlag, 1989. Citado na página [34](#).
- GENES, C. Quantum physics of light-matter interactions. *Lectures for FAU, Max Planck Institute for the science of light*, p. 10–11, 2007. Citado 2 vezes nas páginas [19](#) and [20](#).
- GRIFFITHS, D. J. *Introduction to Quantum Mechanics*. 3. ed. [S.l.]: Pearson Prentice Hall, 2019. Citado 5 vezes nas páginas [9](#), [15](#), [17](#), [23](#), and [26](#).
- GUÉRY-ODELIN, D. et al. Shortcuts to adiabaticity: concepts, methods and applications. *Rev. Mod. Phys.*, v. 91, n. 045001, 2019. Citado 2 vezes nas páginas [26](#) and [27](#).
- HAYASHI, K.; KUGO, T. Everything about weyl's gauge field. *Prog. Theor. Phys.*, v. 61, n. 1, p. 334–346, 1979. Citado na página [19](#).
- HECHT, E. *Optics*. 5. ed. Harlow, England: Pearson, 2017. 588-609 p. Citado na página [13](#).
- HUBER, B. et al. Ghz rabi flopping to rydberg states in hot atomic vapor cells. *Phys. Rev. Lett.*, v. 107, n. 243001, 2011. Citado na página [57](#).
- JACKSON, J. D. *Classical Electrodynamics*. 1. ed. [S.l.]: Wiley, 1998. Citado na página [19](#).
- KATO, T. On the adiabatic theorem of quantum mechanics. *Jour. Phy. Soc. Jap.*, v. 6, n. 435, 2021. Citado na página [23](#).
- KERESZTURY, G. *Handbook of vibrational spectroscopy*. 1. ed. [S.l.]: Wiley, 2002. Citado na página [33](#).
- KEYLON, D. C.; DEPOALA, D. Coherent excitation. *Lectures Notes, REU program, KSU*, n. 4-6, 2015. Citado na página [37](#).
- KUKLINSKI, K. R. et al. Adiabatic population transfer in a three-level system driven by delayed laser pulses. *Phys. Rev. A*, v. 40, n. 11, 1989. Citado 3 vezes nas páginas [14](#), [35](#), and [47](#).
- LAKEHAL, H.; MAAMACHE, M.; CHOI, J. Novel quantum description for nonadiabatic evolution of light wave propagation in time-dependent linear media. *Sci. Rep.*, v. 6, n. 19860, 2016. Citado na página [27](#).
- LI, Y.; CHEN, X. Shortcut to adiabatic population transfer in quantum three-level systems: effective two-level problems and feasible counterdiabatic driving. *Phys. Rev. A*, v. 94, n. 063411, 2016. Citado 6 vezes nas páginas [9](#), [29](#), [30](#), [47](#), [56](#), and [61](#).
- MALINOVSKY, V. L.; KRAUSE, J. L. General theory of population transfer by adiabatic rapid passage with intensified, chirped laser pulses. *Eur. Phys. J. D.*, v. 14, n. 147-155, 2001. Citado na página [26](#).
- MCCREERY, R. L. *Raman spectroscopy for chemical analysis*. 1. ed. [S.l.]: Jon Wiley and Sons, 2000. Citado na página [34](#).
- MEYER, A. et al. Tailoring ultrasonic beams with optoacoustic holography. *Proc. SPIE*, n. 4969, 2003. Citado na página [56](#).

MIE, G. On the absorption of electromagnetic waves. *Ann. der Phys.*, v. 330, n. 3, 1908. Citado na página 33.

POGGIANI G. Z. LI, R.; TESTERA, G.; WERTH, G. Adiabatic cooling of ions in the penning trap. *Phy. Ato. Mol. Clus.*, v. 22, n. 375-382, 1991. Citado na página 26.

RAIMOND, J. M.; BRUNE, M.; HAROCHE, S. Manipulating quantum entanglement with atoms and photons in a cavity. *Rev. Mod. Phys.*, v. 73, n. 565, 2001. Citado na página 13.

RAMAN, C. V. A new radiation. *Ind. Jour. Phys.*, v. 2, n. 387-398, 1928. Citado na página 33.

RIBEIRO, W. L.; LANDI, G. T.; SEMIÃO, F. L. Quantum thermodynamics and work fluctuations with applications to magnetic resonance. *Am. J. Phys.*, v. 84, n. 948-957, 2016. Citado na página 64.

ROYCHOWDBURY, A.; DEFFNER, S. Time-rescaling of dirac dynamics: Shortcuts to adiabaticity in ion traps and weyl semimetals. *Entropy*, v. 23(1), n. 81, 2021. Citado na página 32.

SAKURAI, J. J.; NAPOLITANO, J. *Modern Quantum Mechanics*. 3. ed. [S.l.]: Cambridge University Press, 2021. Citado 2 vezes nas páginas 25 and 66.

SANTOS, A. C.; D., S. R.; SARANDY, M. S. Shortcut to adiabatic gate teleportation. *Phys. Rev. A*, v. 93, n. 012311, 2016. Citado na página 13.

SANTOS, A. F. d. et al. Influence of polarization and the environment on wave-particle duality. *Quan. Inf. Proces.*, v. 22, n. 63, 2023. Citado 2 vezes nas páginas 13 and 26.

SCHLOSSHAUER, M. *Decoherence and the Quantum-To-Classical Transition*. 1. ed. [S.l.]: Springer, 2007. Citado na página 26.

SHANKAR, R. *Principles of Quantum Mechanics*. 1. ed. [S.l.]: Kluwer Academic/ Plenum Publishers, 1994. Citado 2 vezes nas páginas 17 and 19.

SHIMADA, K. et al. Spectrum shuttle for producing spatially shapable ghz burst pulses. *Adv. Pho. Nex.*, v. 3, n. 016002, 2023. Citado na página 57.

SHORE, B. W. Picturing stimulated raman adiabatic passage: a stirap tutorial. *Adv. Opt. Phot.*, v. 9, n. 563-719, 2017. Citado 7 vezes nas páginas 10, 14, 35, 43, 45, 47, and 60.

STRUTT, J. W. On the light from the sky, its polarization and colour. *The Lon. Edim. and Dub. Phylo. Mag. and Jour. Sci.*, v. 41, n. 271, 1871. Citado na página 33.

SUTER, D.; ALVAREZ, G. A. Protecting quantum information against environmental noise. *Rev. Mod. Phys.*, v. 88, n. 041001, 2016. Citado na página 26.

THAKURIA, D. et al. Generalised quantum speed limit for arbitrary time-continuous evolution. *J. Phys. A: Math. Theor.*, v. 57, n. 025302, 2024. Citado na página 57.

TORRONTEGUI, E. Energy consumption for shortcuts to adiabaticity. *Phys. Rev. A*, v. 96, n. 022133, 2017. Citado na página 27.

- TORRONTGUI, E. et al. Shortcuts to adiabaticity: Fast-forward approach. *Phys. Rev. A*, v. 86, n. 013601, 2013. Citado na página 27.
- UHLMANN, A. An energy dispersion estimate. *Phys. Lett. A*, v. 161, n. 329, 1992. Citado na página 57.
- VITANOV, N. V. et al. Coherent manipulation of atoms and molecules by sequential laser pulses. *Adv. Atom. Mol. Opt. Phys.*, v. 46, 2001. Citado 5 vezes nas páginas 14, 35, 43, 45, and 47.
- VITANOV, N. V. et al. Stimulated raman adiabatic passage in physics, chemistry and beyond. *Rev. Mod. Phys.*, v. 89, n. 015006, 2017. Citado 3 vezes nas páginas 14, 35, and 43.
- VOLYA, D.; MISHRA, P. State preparation on quantum computers via quantum steering. *Trans. Quan. Eng.*, v. 5, n. 3100714, p. 1–14, 2024. Citado na página 13.
- WANG, Y. et al. Realization of population inversion between $7s_{1/2}$ and $6p_{3/2}$ levels of cesium for four-level active optical clock. *Sci. China Phys. Mech. Astron.*, v. 56, n. 1107-1110, 2013. Citado na página 13.
- YAMAGUCHI, J. et al. Estimation of shor’s circuit for 2048-bit integers based on quantum simulator. *Cryptology ePrint Archive*, n. 2023/092, 2023. Citado na página 14.
- YIN, Z. et al. Shortcuts to adiabaticity for open systems in circuit quantum electrodynamics. *Nat. Comm.*, v. 13, n. 188, 2022. Citado na página 26.
- YONEDA, J. et al. Coherent spin qubit transport in silicon. *Nat. Comm.*, v. 12, n. 4114, 2021. Citado na página 13.
- ZHOU, H. et al. Floquet-engineered quantum state transfer in spin chains. *Sci. Bul.*, v. 64, n. 13, 2019. Citado na página 29.
- ZWIEBACH, B. Lectures on quantum physics iii. MIT Open Course Ware, p. 73–77, 2018. Citado na página 17.